UNH-

NEUTRON MEASUREMENTS on the OGO-VI Spacecraft

FINAL SCIENTIFIC REPORT
NASA Contract NAS 5-9313
NASA Grant NGR 30-002-088

J. A. Lockwood
Principal Investigator

Space Science Center
Department of Physics
UNIVERSITY OF NEW HAMPSHIRE
Durham

NEUTRON MEASUREMENTS on the OGO-VI Spacecraft

FINAL SCIENTIFIC REPORT
NASA Contract NAS 5-9313
NASA Grant NGR 30-002-088

J. A. Lockwood
Principal Investigator

University of New Hampshire
Space Science Center
Department of Physics
Durham, New Hampshire 03824

NATIONAL AERONAUTICS AND SPACE ADMINISTRATION

January 1973

ACKNOWLEDGMENTS

The co-investigators on this project were:

Dr. R. Jenkins
Communications Research Center
Ottawa, Ontario
Canada

Dr. E. Chupp
Physics Department
University of New Hampshire
Durham, New Hampshire 03824

We are grateful to the following people who have worked on various phases of this project:

Archer Buck
Richard Simmons
Bea Day
H. Razdan
S. Dewdney
Larry Friling
Daniel Huntley
Susan Whitcomb
Albert Knight
W. Dotchin

The following Ph.D. student was supported under this project and completed his Ph.D. dissertation:

Shadrach Ifedili

The detection system was designed and constructed by Time-Zero, Inc., and the extra efforts of G. Spellman, R. Hill, and the staff of Time-Zero to make the flight successful were greatly appreciated.

TABLE OF CONTENTS

1. INTRODUCTION

The principle emphasis in this project has been upon the following specific tasks:

(1) The design and calibration of a neutron monitor to measure the cosmic-ray neutron leakage from the earth's atmosphere at altitudes from 400 to 1000 km over a range of latitudes from $0<\lambda<90^{o}$.

(2) To determine latitude dependence of the cosmic-ray leakage flux.

(3) Measure the altitude dependence of the cosmic ray neutron leakage flux.

(4) Measure the energy spectrum of the cosmic-ray neutron leakage flux in the energy range from .01 to 10 MeV.

(5) To search for solar neutrons during both quiet times and solar flare events.

(6) To evaluate the neutron flux from the interaction of solar protons in the polar latitudes.

(7) To determine the angular distribution of the neutron leakage flux as deduced by measurements of the altitude dependence.

(8) Verify the solar modulation of the cosmic-ray source for the neutron leakage.

There has been no attempt yet to study the following problems:

(1) The magnitude and fluctuation of energetic charged particles over the poles.

Since the detector on OGO-VI had charged-particle detectors with a very large geometrical factor, we can determine the fluctuations in the low-energy charged-particle fluxes over both poles. Such fluctuations are associated with geomagnetic cutoff perturbations and solar proton fluxes. So far no attempt has been made to unravel these affects.

(2) The anisotropies in the protons above about 70 MeV. This can be measured using the coincidence banks in the charged particle detector array. However, no studies have been made. Again the results should be rather interesting because our detector efficiency is large. We have observed charged-particle anisotropies when the detector passes into the South Atlantic magnetic anomaly. Only a preliminary investigation has been made. This was done because these data from the anomaly must be eliminated from our analyses of the cosmic ray neutron leakage flux measurements. During such passes there is a large amount of neutron production affects by the energetic protons trapped at these altitudes.

(3) Short duration counting-rate bursts. These might be present in the charged-particle data from solar x-ray fluxes incident on the detector. This is a large task and involves reworking the primary data tapes. It does not, however, seem warranted at this point.

Since most of the proposed analyses for this project have been published, we have included several reprints in this report. Other results are already in preprint form, copies of which are attached, or are contained in a Ph.D. dissertation by S. Ifedili. We have not included any discussion of the details of the design criteria, the methods of construction of the neutron detector, nor of the calibration at various particle-accelerator facilities and with radioactive sources. These details can be found in the final technical report of Time-Zero,Inc., on this project.

2. COSMIC-RAY NEUTRON MONITOR FOR OGO-VI

The objective of this experiment is to monitor the cosmic-ray neutron flux over a large region of space near the earth for an extended time with a simple neutron monitor. The basic detecting system to measure the integrated neutron flux from 10^{-8} to 15 MeV consists of a moderated He^3 proportional counter surrounded by a charged-particle rejection system. A plastic scintillator viewed by a photomultiplier is operated in coincidence with the neutron counter to determine the energy spectrum and flux in the 1-10 MeV range. In order to minimize contributions from neutrons produced within the OGO spacecraft, the sensor is located about 4.5 meters out on the EP-5 boom. The experiment includes an in-flight calibrator to check pulse discriminator levels on neutron and charged-particle channels and a calibration-loop system to compensate for changes in the photomultiplier gain. The mean neutron detection efficiency for the expected neutron energy spectrum over the energy range 10^{-8}-15 MeV is 1.8 cm^2. The weight of the neutron sensor is 2.58 kg, with a length of 0.314 meter and a diameter of 0.111 meters. The total power requirements are 4.5 watts.

(IEEE Transactions on Geoscience Electronics, Volume GE-7, Number 2, April 1968, pp. 88-93.)

The details of the design and testing of the detector are contained in Appendix 1, page A-1.

3. LATITUDE AND ALTITUDE DEPENDENCE OF THE COSMIC RAY NEUTRON LEAKAGE FLUX

Preliminary measurements of the cosmic ray albedo neutron flux above 400 km are reported for the period June 7 to 17, 1969. The measurements were made with a detector on board the OGO-6 satellite that responds primarily to neutrons in the energy range 10^4 to 10^6 ev. The latitude variation of the counting rate was found to be 7.4/1 between 90° and 0°, similar to that predicted by Lingenfelter (1963). The neutron counting rate near the poles was found to decrease by 26±5% between 450 and 950 km altitude, corresponding to a $R^{-4.2\pm0.9}$ dependence, where R is the distance from the center of the earth. This large altitude dependence excludes any angular distributions of neutron flux at the top of the atmosphere that are more peaked toward the vertical than cos θ (where θ is the angle from the vertical), but it is not in

disagreement with an isotropic neutron flux. The total neutron leakage flux found by assuming isotropy was about 0.7 times that predicted by Lingenfelter (1963). The neutron leakage flux values obtained from the OGO 6 experiment agree with those estimated from other experiments with a similar neutron energy response, if the same angular distribution is used. Estimates of the total neutron leakage flux, deduced from experiments responsive only to neutrons above 1 MeV by using the Lingenfelter (1963) and Newkirk (1963) energy spectra of leakage neutrons, show agreement with the lower energy results when the Newkirk spectrum is used but are up to twice as great as the lower energy results when the Lingenfelter spectrum is applied.

(Journal of Geophysical Research, Volume 75, No. 22, page 4197, 1970.)

The details of the results on the latitude and altitude dependence of the cosmic ray albedo neutron flux are contained in Appendix II, page A2.

4. ENERGY DEPENDENCE OF THE COSMIC RAY NEUTRON LEAKAGE FLUX IN THE RANGE .01 TO 10 MeV

The cosmic-ray neutron leakage flux and energy spectrum in the range 1-10 MeV were measured by a neutron detector on the OGO 6 satellite from June 7 to September 30, 1969. The same detector simultaneously measured the total leakage flux, having 75% of its response to the leakage flux in the interval 1 keV to 1 MeV. For a neutron energy spectrum of the form $AE^{-\gamma}$ in the range 1-10 MeV, the upper limit to γ for polar regions ($P_c < 0.3$ Gv) was found to be 1.0 and for the equatorial regions ($P_c > 12$ Gv) was 1.2. For the polar regions, the lower limit to γ was found to be 0.8. This energy spectrum at 1-10 MeV is slightly flatter than L. L. Newkirk predicted. The neutron fluxes at 1-10 MeV were 0.28±0.03 and 0.035±0.003 $cm^{-2}sec^{-1}$ for $P_c < 0.3$ and $P_c > 12$ Gv, respectively. The ratios of the neutron flux at 1-10 MeV to the total neutron flux were 0.54±0.07 for $P_c > 0.3$ Gv and 0.50±0.06 for $P_c > 12$ Gv.

(Journal of Geophysical Research, Vol. 76, No. 31., Page 7470, 1971.)

The details of the analysis of the energy dependence of the neutron leakage flux are contained in Appendix III, page A3.

5. UPPER LIMIT TO THE 1 TO 20 MEV SOLAR NEUTRON FLUX

The upper limit on the quiet time solar neutron flux from 1-20 MeV has been measured to be less than 2×10^{-3} n/cm^{2}sec at the 95% confidence level. This result is deduced from the OGO-VI neutron detector measurements of the "day-night" effect near the equator at low altitudes for the period from June 7, 1969 to December 23, 1969. The OGO-VI detector had very low (<4%) counting rate contributions from locally produced neutrons in the detecting system and the spacecraft and from charged-particle interactions in the neutron sensor.

(Submitted to Solar Physics for publication).

The details of these searches for neutrons are contained in Appendix IV, page A4.

6. A SEARCH FOR SOLAR NEUTRONS DURING SOLAR FLARE EVENTS

During the operational period of the experiment from June 7 to December 23, 1969, several large solar flares occurred. No solar neutron flux was positively identified in the time association with large flare events in this time period. Hence, only upper limits to the solar neutron flux can be discussed. The results have been compared with the models for the solar neutron production during the solar flares proposed by Lingenfelter (1963) and the Lingenfelter and Ramaty (1967). The details of the observations of the optical activity for the flares considered are in Table 5 and the solar proton emission in Table 6. Proton data were available for all the solar flares. For the large event on November 2, the data from Masley (1972) enabled us to determine the form of the energy spectrum using the exponential rigidity function. J_o was 8.50×10^4 protons/cm^2 sec ster., and $(dJ/dP)_o = J_o/P_o = 1850$ protons per cm^2 sec ster. M/v. P_o was approximately 50 MV.

TABLE 5

OPTICAL ACTIVITY

Optical Flare(1969)	Importance	Position	Onset Time(ut)	End (ut)	Time of Max(ut)
June 13	3B	S24E69	15.49	20.00	16.33
June 15	2N-2B	S17W77	08.31	08.50	08.40
Sept 25	2N-3N	N14W14	07.00	08.53	07.24
Nov 02	3B	N22W90	10.28	11.57	11.39
Dec 19	1N-2 F	N10W08	12.01	12.40	12.20

TABLE 6

SOLAR PROTON EMISSION (EXPLORER 41)

Date(1969)	Solar Proton Flux (ster cm^2 sec)$^{-1}$			Peak time
	>60MeV	>30MeV	>10MeV	
Sept 25	0.2	1	15	∿11.00
Nov 02	39	257	1437	12.00-13.00
Dec 20	0.6	1.1	8.3	∿01.00

The data used for this study were the gated neutron count rates for the OGO-VI detector on the sunward side of the earth. No background corrections were made because only the differences in counting rates were used. Only neutron rates corresponding to charged-particle rates less than 1.5 times the mean for that vertical cutoff rigidity were included in the analysis. To exclude solar-proton produced leakage neutrons we restricted the solar neutron analysis to geomagnetic latitudes less than 30^{o}. The neutron data were also selected from altitudes less than 900 kilometers to reduce neutron production effect by the energetic protons trapped in the inner radiation belt.

Lingenfelter and Ramaty (1967) proposed that solar neutrons would arrive at the earth monoenergetic in time if the neutrons were emitted impulsively from the sun in a time interval which is comparable with the rise time of the optical flare. For these assumptions they calculated the time dependence neutron flux at the earth considering that neutrons will be produced both during the acceleration and the slowing down phases of the solar flare. The data which we selected were on the basis of the time dependency of the solar neutron flux as predicted by this model. For the large solar flare event on November 2, we found no statistically significant difference in the counting rates during the flare event and another pass through the same region when there would be no solar neutrons. For this event the upper limit to the solar neutron rate is 5.0×10^{-2} counts/sec at the 95% confidence level. The corresponding upper limit to the solar

neutron flux is 0.135 neutron/cm^2 per sec. If these results are corrected for the atmospheric solar neutron leakage flux arising from the interaction of solar neutrons with the earth's atmosphere the upper limit is now 5×10^{-2} neutrons/cm^2 per sec in the 1-20 MeV energy range.

Comparing this upper limit with the predicted solar neutron flux using the Lingenfelter model (1969), we find that the calculations predict a neutron flux at earth at approximately 0.21 neutrons/cm^2 per sec. Noting that only about 27% of all the solar neutrons predicted by Lingenfelter are in the 1-20 MeV energy range, the maximum major upper limit to the total solar neutron flux from our measurements is 0.19 neutrons/cm^2 per sec. These observations, therefore, are consistent with this model. In other words, this upper limit is within agreement with Lingenfelter's prediction. This does not imply that there is a detectable solar neutron flux. For the other solar flare events on September 25, December 19, June 13, and June 15, upper limits to the solar neutron flux can also be obtained, not inconsistent with theoretical predictions. This we believe is the first time that an upper limit to a solar neutron flux has been measured for a flare of importance greater than 3B. We must emphasize that our measurements do not suggest that there are any solar neutrons from impulsive flare events. Perhaps only when larger detectors with better efficiency and directionality are flown will it be possible to determine if there are any solar neutrons.

7. SOLAR PROTON NEUTRON LEAKAGE MEASUREMENTS

Energetic solar protons incident on the earth's atmosphere at high latitudes will produce neutrons, some of which will produce neutrons, which will then leak out of the atmosphere. A fraction of these leakage neutrons will travel in directions such that the radioactive decay of the neutrons into protons and electrons occurs within the magnetosphere. Consequently, the protons and electrons can become trapped. Hence, this may be one source of the energetic protons in the radiation belts. The neutron data from the OGO-VI satellite enabled us to evaluate the solar proton production of neutrons during several flare events.

The neutron counting rates were derived from those events in the ^{3}He proportional counter not associated with the charged-particle guard counter events. These gated neutron counting rates were selected for geomagnetic latitudes λ (north and south) leakage (greater than 70°) because the solar protons giving rise to the neutron are restricted to the polar regions of the earth. In most flare events the protons have kinetic energies less than about 300 MeV. Consequently, the effects of the solar protons will not be seen at latitudes less than 70°. The neutron counter rates were then corrected for dead time and reduced to a common altitude of 450 km using the observed altitude dependence discussed in Section 3. The details of the optical observations, riometer absorptions, and the solar proton emissions are summarized in Tables 1 and 2

TABLE 1

SOLAR FLARE EVENTS

Date (1969)	Onset Time (ut)	End (ut)	Time of Maximum (ut)	Importance	Solar Region	Max Riometer Absorption db at 30mHz
Sept 25	0700	0853	0724	2N-3N	N14W14	0.7
Nov 02	1028	1157	1139	3B	N22W90	14.5
Nov 24	0913	1000	0918	2B-3N	N16W32	0.7
Dec 18	0745	0826	0725	1N-2F	N15E28	0.6
Dec 19	1201	1240	1220	1N-2F	N10W08	1.3

TABLE 2

SOLAR PROTON EMISSION (EXPLORER 41)

Date (1969)	Proton flux (ster cm s)$^{-1}$			Time of Peak flux (ut)
	>60Mev	>30Mev	>10Mev	
Sept 25	0.2	1	15	~11.00
Nov 02	39	257	1437	12.00-13.00
Nov 24	0.4	0.9	3.5	~17.00
Dec 18	0.6	1.2	1.5	~20.00
Dec 20	0.6	1.1	8.3	~01.00

for the solar flares of September 25, November 24, December 18, and December 19. Coincident with the proton flux enhancements recorded on Explorer 41 are the transient increases in the gated neutron rates above the cosmic ray albedo neutron rate background (Figures 1, 2, 3, 4).

To compare our results with the calculations of Lingenfelter and Flamm (1964) on the neutron leakage flux produced by solar protons we must have data on the energy spectra and charge composition of the energetic solar particles. Furthermore, we must make background corrections to the observed neutron counting rates. This also necessitates data on the solar particle composition and energy spectra. The method to make these background corrections is straight-forward and is discussed by Jenkins et.al. (1971). As an example of the background corrections we tabulate the contributions to the neutron rates of the ^3He counter at the poles for the September 25, 1969, solar flare event (Table 3).

After making the necessary background corrections for local production and non-neutron events, we obtain 0.18±0.05 counts/sec as the actual increase of the neutron counting rate at 450 km for the solar event on September 25. This corresponds to a neutron counting rate of 0.23±0.06 counts/sec at the top of the atmosphere (taken to 50 km altitude). Therefore, the neutron leakage flux from solar protons is 0.11±0.03 neutrons/cm^2 sec. From the measurements of the solar proton energy spectrum (Masley, 1972) we obtained a relation between the integral proton flux J and the rigidity of the protons P

TABLE 3

CORRECTIONS TO THE He^3-COUNTER GATED NEUTRON COUNTING RATE (CTS/SEC) AT THE POLES FOR THE SEPTEMBER 25, 1969 SOLAR FLARE EVENT

Locally produced neutrons	
In the spacecraft mainbody	0.0052
In the EP5 set up	0.0016
In the neighboring electronics and detector walls	0.0576
In the moderator	0.0009
Highly ionizing events in the He^3 counter	
Low-energy solar protons	0.0000
Low-energy solar α particles	0.0000
Z >2 solar cosmic rays (including showers)	0.0000
Evaporation protons from solar cosmic ray interactions	0.0004
Proton and α-initiated shower particles	0.0000
Total Correction	0.0657

which agreed with the Explorer 41 proton data using the relationship $J = J_o \exp(-P/P_o)$ and $(dJ/dP)_o$. We found that the characteristic rigidity of the solar protons, P_o, was 57 Mv and the total directional intensity of solar protons near the earth J_o was 60.4 $(cm^2 \text{ sec ster})^{-1}$. For this solar proton rigidity spectrum the calculations of Lingenfelter and Flamm (1964) predict a neutron leakage flux of = 0.085 neutrons/cm^2 sec. Our result, therefore, is in reasonable agreement with the theoretical predictions for this flare event.

We also studied the November 24, December 18, and December 19, solar proton events. The results are listed on Table 4. For these flares, however, the energy spectrum and charge composition of the solar particles were not available. We, therefore, assumed a power-law energy dependence and used the proton data of Explorer 41 on the integral flux greater than 60 MeV and greater than 30 MeV to estimate the integral and differential energy spectra. From Table 4, we see that the measured neutron leakage fluxes for the November 24, December 18, and December 19 solar-proton events are in reasonable agreement with the theoretical predictions.

The measurement of the solar-proton neutron leakage at low latitudes is important because only the neutron decay products injected at low latitudes can contribute to the inner zone protons. The data used for the low latitude study were the gated neutron rates at geomagnetic latitudes both north and south, less than 45^o. This selection minimizes the contributions from local production of neutrons by charged particle

TABLE 4

COMPARISON OF THE MEASURED AND PREDICTED SOLAR PROTON ALBEDO NEUTRON FLUX

Date of the Solar proton event (1969)	The Characteristic rigidity of the solar protons, P_o (MV)	Total directional intensity of the solar protons, J_o ($cm^2 sec\ ster)^{-1}$	Solar proton albedo neutron rate at 450km altitude cts/sec	Solar proton albedo neutron flux at the top of the polar atmosphere (50 km) $cm^{-2}sec^{-1}$	
				Measured	Predicted
September 25	57	60.4	0.18±0.05	0.11 ±0.03	0.085
November 24	113	6.83	0.21±0.09	0.12 ±0.05	0.02
December 18	130	6.96	0.11±0.05	0.063 ±0.028	0.030
December 19	148	5.21	0.13±0.05	0.074 ±0.029	0.035

interacting with the satellite assembly and unshielded portions of the detector. The neutron counting rates corresponding to charged particle rates greater than 1.5 times the minimum value for the particular cutoff rigidity were excluded from the analysis. The rates were selected for small intervals of latitude and altitude to avoid any latitude or altitude bias for the time intervals involved. There were no measureable Forbush decreases or other time-variations in the cosmic-ray source which would produce uncertainties in the interpretation of the results. As an example we show in Figure 5 the neutron rates for the September 25, 1969 event. There was no apparent enhancement in the neutron counting rates at low latitudes during the event. On the other hand for November 2, 1969 (Figure 6) there appears to be an enhancement in the neutron rates which is time associated with the solar-proton flux at high latitudes. Following the analysis of Lingenfelter and Flamm (1964) we can deduce the predicted neutron flux at low latitudes. The predicted neutron leakage rate at 42^{o} geomagnetic latitude and 750 km altitude is 0.21 counts/sec. This result is within the two standard deviations of the observed rate. For all the other events the predicted solar-proton neutron leakage fluxes at low latitudes were within the statistical uncertainties of the data, which for the known solar proton flux and energy spectra, agree with the theoretical predictions.

Now let us investigate the possibility that the brief neutron increase on November 2 is from sources other than the solar proton albedo neutrons. First, the results on the

solar neutron flux (Section 5) indicate that it cannot be due to this source. No detectable solar neutron flux has been observed. Second, local production could not have produced the neutron enhancement because the charged particle rates were essentially the same as had been observed during previous passes through the same region. Third, any cutoff rigidity change from magnetic field perturbations can not be a cause for the enhanced neutron rates. Finally, it is unlikely that alpha particles could have made any significant neutron contributions. This is based on known proton-to-alpha ratios for the November 2 solar flare event. Therefore, for the November 2 event we must conclude that the brief neutron enhancement was presumably due to polar cap protons producing neutrons which then travelled to lower latitudes.

8. THE ANGULAR DISTRIBUTION OF THE NEUTRON LEAKAGE FLUX AS DEDUCED FROM THE ALTITUDE DEPENDENCE

The altitude variation of the neutron counting rate above the atmosphere is related to the angular distribution of the leakage neutrons as follows: The counting rate of the neutron detector above the earth's atmosphere neglecting neutron decay is given by:

(1) $$N = \int_{4\pi} d(\vec{\Omega})\ \varepsilon\ (\vec{\Omega})\ \phi_o\ (\vec{\Omega})$$

where $\varepsilon\ (\Omega)$ is the efficiency of the detector (counts/neutron/cm^2) for neutrons arriving in the direction r at the detector. The neutron flux $\phi_o\ (\Omega)$ in the direction Ω at the spacecraft is the same as the neutron flux $\phi\ (\Omega)$ at the top of the atmosphere if the direction ($-\Omega$ measured from the detector) intersects the top of the atmosphere. Otherwise the flux is zero. We can write the neutron counter rate as follows

(2) $$N = \int dA\ \varepsilon\ (\vec{\Omega})\ \phi\ (\theta)\ k(\nu)\ \frac{\cos\nu}{r^2}$$

where the integration is over the top of the atmosphere visible to the detector and ϕ has been written as a separable function in θ and ν. These relationships are illustrated in Figure 7 where we have indicated the spacecraft location and a sample point at the top of the atmosphere. In evaluating the above equation the variables were written in terms of height h above the top of the atmosphere, the geomagnetic colatitude and geomagnetic longitude. (The detailed calculations are presented in the Ph.D. dissertation by S. Ifedili). In this analysis we must

keep in mind that the latitude dependence of the counting rate is much larger than the altitude dependence of the counting rate at any given latitude. Therefore the effects of latitude mixing upon the altitude dependence are very important.

From the mean latitude and altitude dependence of the counting rates we can deduce the form of the angular distribution for the neutron leakage in the energy range from .01 - 10 Mev. The neutron counting rates were again derived from the ^3He proportional counter events not associated with counts in the charged-particle guard counters. Contributions from local production were minimized by taking neutron counting rates corresponding to charged-particle rates less than twice the minimum values for the particular vertical cutoff rigidity. Data acquired in the regions near the Cape Town and Brazilian anomalies were excluded as well as data from excursions into the horns of the outer radiations belt.

We must recognize that any error in the rigidity location or in the vertical cutoff rigidity might contribute an error to the altitude variation of the neutron intensity. Hence, we evaluated such contributions carefully. However, if each location in a rigidity bin contributed equally at all altitudes the errors would be a minimum. This is generally the situation when the period of analysis equals the time taken for the satellite's orbit to progress through 360°. This was approximately 4 months for the OGO-VI satellite. So the time period selected for the study was June 7 to September 30, 1969. The results of the altitude dependence are summarized in Table 7. The changes in the altitude

TABLE 7

THE ALTITUDE DEPENDENCE OF THE ALBEDO NEUTRON FLUX

Rigidity range(GV)	Geomagnetic latitude degrees	Neutron Rate Percentage change $\frac{N_{450}-N_{1050}}{N_{450}} \times 100\%$	Power law, $R^{-\beta}$ (R is distance from center of earth)
0- 0.3	80.0	25.3±1.1	$R^{-3.45\pm0.18}$
0.3- 0.6	68.0	26.8±1.1	$R^{-3.68\pm0.18}$
1.5- 2.0	55.0	27.6±1.4	$R^{-3.83\pm0.23}$
2.0- 2.5	52.0	28.0±1.1	$R^{-3.89\pm0.17}$
2.5- 3.0	49.5	27.3±1.0	$R^{-3.78\pm0.16}$
3.0- 3.5	47.0	25.7±1.0	$R^{-3.51\pm0.16}$
3.5- 4.0	45.0	23.1±1.1	$R^{-3.11\pm0.17}$
4.0- 5.0	42.5	24.2±1.0	$R^{-3.27\pm0.15}$
5.0- 6.0	39.5	22.4±1.1	$R^{-3.01\pm0.16}$
6.0- 7.0	37.0	20.3±1.3	$R^{-2.68\pm0.19}$
7.0- 8.0	35.0	19.4±1.4	$R^{-2.55\pm0.20}$
8.0-10.0	31.5	21.1±1.1	$R^{-2.80\pm0.17}$
10.0-12.0	26.5	18.5±1.3	$R^{-2.41\pm0.19}$
12.0-14.0	20.0	18.1±1.4	$R^{-2.36\pm0.20}$
14.0-16.0	7.5	21.0±1.4	$R^{-2.79\pm0.20}$
>16.0	0.0	20.3±1.6	$R^{-2.69\pm0.23}$

dependence of the neutron leakage flux with latitude are attributed to the shape of the latitude variation of the neutron flux and the effects of latitude mixing, recognizing that the detector sees neutrons from a wider range of latitudes as the altitude increases. We must remember that the neutron leakage flux starts to increase rapidly with latitude (Appendix II) at about 20°, increases steadily until about 55° when it flattens and is latitude independent above 55°. Hence, we would expect that at about 20° latitude, the higher altitudes, which include a larger range of geomagnetic latitudes, would be affected by the latitude mixing. At about 20° we would expect a minimum altitude change in the neutron counting rate. Similarly we expect a maximum altitude change for counting rates at locations greater than 55° when the counting rates are independent latitudes. This is exactly as observed.

The percentage change in the counting rate as a function of geomagnetic latitude is shown in Fig. 8. The calculated altitude changes are indicated for different assumed angular distributions of the neutron leakage. The results shown suggest that the angular distribution of the neutron leakage at the top of the atmosphere is essentially isotropic. The best fit of the observed to the predicted altitude dependence at $\lambda < 60^{\circ}$ is for an isotropic angular distribution $k(\nu)=1$. Angular distributions which are peaked more to the vertical or to the horizontal do not agree as well with the observed altitude dependence. The better statistics in the polar regions enable us to make a better comparison of the calculated and measured altitude dependence of the

neutron rates. For $\lambda > 60^{o}$ the angular distribution is given by $k(\nu) = 1 - 0.5 \cos \nu$, although an isotropic angular distribution is not in disagreement with the observations. The somewhat flatter (or pancake-shaped) angular distribution at the poles might be due to the enrichment of the neutron energy spectrum preferentially in the high energy region. These high-energy neutrons would be very strongly peaked in the forward direction, being largely the result of knock-on collisions in the thicker atmosphere for which the neutrons travel near the horizontal direction. However, they have to be degraded in energy to less than 10 Mev in order to be detected by the OGO-VI sensor. From a survey of elastic high-energy neutron interactions, considerable peaking of the scattered neutrons in the forward direction is observed. Therefore, mixture of an isotropic high-energy neutrons degraded to less than 10 Mev (about 4%) with a preponderant fraction of evaporation neutrons (about 96%) might explain the flatter angular distribution in the polar region.

9. SOLAR MODULATION OF THE COSMIC RAY NEUTRON LEAKAGE FLUX.

The solar modulation of the cosmic rays should be reflected in the production of neutrons in the atmosphere of the earth. The effects of such a modulation would be observed in the rapid transient decreases (Forbush decreases) and in the 11-year variation which is anticorrelated with the 11-year sunspot cycle. For a typical cosmic ray detector such as a neutron monitor the amplitude of the 11-year variation is about 20-30% and is energy dependent. The low energy particles are more strongly modulated.

Lingenfelter (1963) calculated the energy, latitude and altitude distributions for the neutron leakage at the minimum and maximum of the solar activity cycle.

To check these predictions for the 11-year variation we must make certain that the data being used are free from all other variations. There should be no measureable Forbush decreases, no polar-cap neutron events, no observable solar neutrons, and no neutron production affects from radiation-belt protons. For the study we selected the months of July and October, 1969. During this period the Mt. Washington neutron monitor increased about 4%, which is one-fifth of the complete solar cycle variations. The OGO-VI data used were the ^{3}He gated neutron counting rates at 400-500 km altitude, excluding data acquired in the regions of the Capetown and Brazilian anomolies. The neutron counting rates were used only when the associated total charged particle rates were less than twice the minimum at that location. The neutron rates were also corrected for dead time, for locally produced neutrons, and highly ionized charged-particles using the techniques described in Appendix II.

The results are shown in Figure 9. Assuming that any latitude the change in the neutron leakage flux as calculated by Lingenfelter was a linear function of the cosmic-ray intensity as measured by a neutron monitor at low cutoff rigidities, we could predict the neutron leakage rates for the months of July and October, 1969. We normalized the predicted neutron leakage flux to the observed ^{3}He count rates for July. From Figure 9

it is evident that the measurements are in reasonable agreement with Lingenfelter's calculations for the 11-year solar modulation, although the change for this time period is small. It appears that Lingenfelter's calculations can be used with much greater confidence to correct the observed neutron fluxes for the 11-year modulation which is necessary for comparison of the neutron fluxes measured at different epochs in the solar-activity cycle. We attempted to determine the effects of Forbush decreases on the cosmic-ray neutron leakage. Again the same criteria were applied in selecting the ^{3}He events. But, as Forbush decreases generally last only a few days, it is very difficult to make accurate comparisons with the large statistical errors present in the neutron data. A series of two successive Forbush decreases which occurred in November, 1969, provided an opportunity to make limited comparisons. From this comparison we concluded that the cosmic-ray neutron flux ($E<10$Mev) at $\lambda>60^{o}$ was depressed slightly during the Forbush decreases. However, the short duration of the Forbush decrease indicated that intergrated effects on the cosmic-ray neutron leakage are insignificant.

10. REFERENCES

Jenkins, R. W., S. O. Ifedili, J. A. Lockwood, and H. Razdan, J. Geophys. Res. 16, 7470, 1971.

Lingenfelter, R. E., J. Geophys. Res. 68, 5633, 1963.

Lingenfelter, R. E. and E. J. Flamm, J. Geophys. Res. 69, 2199, 1964.

Lingenfelter, R. E. and R. Ramaty, 1967 High Energy Nuclear Reactions in Astrophysics, p. 99 (ed. B.S.P. Shen, W. A. Benjamin, Inc., N.Y.).

Lingenfelter, R. E., Solar Physics 8, 341, 1969.

Masley, A. J., Private communication, 1972.

11. FIGURE CAPTIONS

Figure 1 - Neutron rates at geomagnetic latitude $\lambda > 70^{o}$ during the September 25 solar proton event.

Figure 2 - Neutron rates at $\lambda > 70^{o}$ during the November 24 solar proton event.

Figure 3 - Neutron rates at $\lambda > 70^{o}$ during the December 18 solar proton event.

Figure 4 - Neutron rates at $\lambda > 70^{o}$ during the December 19 solar proton event.

Figure 5 - Neutron rates at low geomagnetic latitudes during the September 25 solar proton event.

Figure 6 - Neutron rates at low geomagnetic latitudes during the November 2 solar proton event.

Figure 7 - The geometry for calculating the angular dependence of the neutron leakage flux from the altitude variation of the observed neutron counting rate.

Figure 8 - The angular dependence of the cosmic-ray neutron leakage flux.

Figure 9 - The 11-year modulation of the cosmic-ray neutron leakage flux.

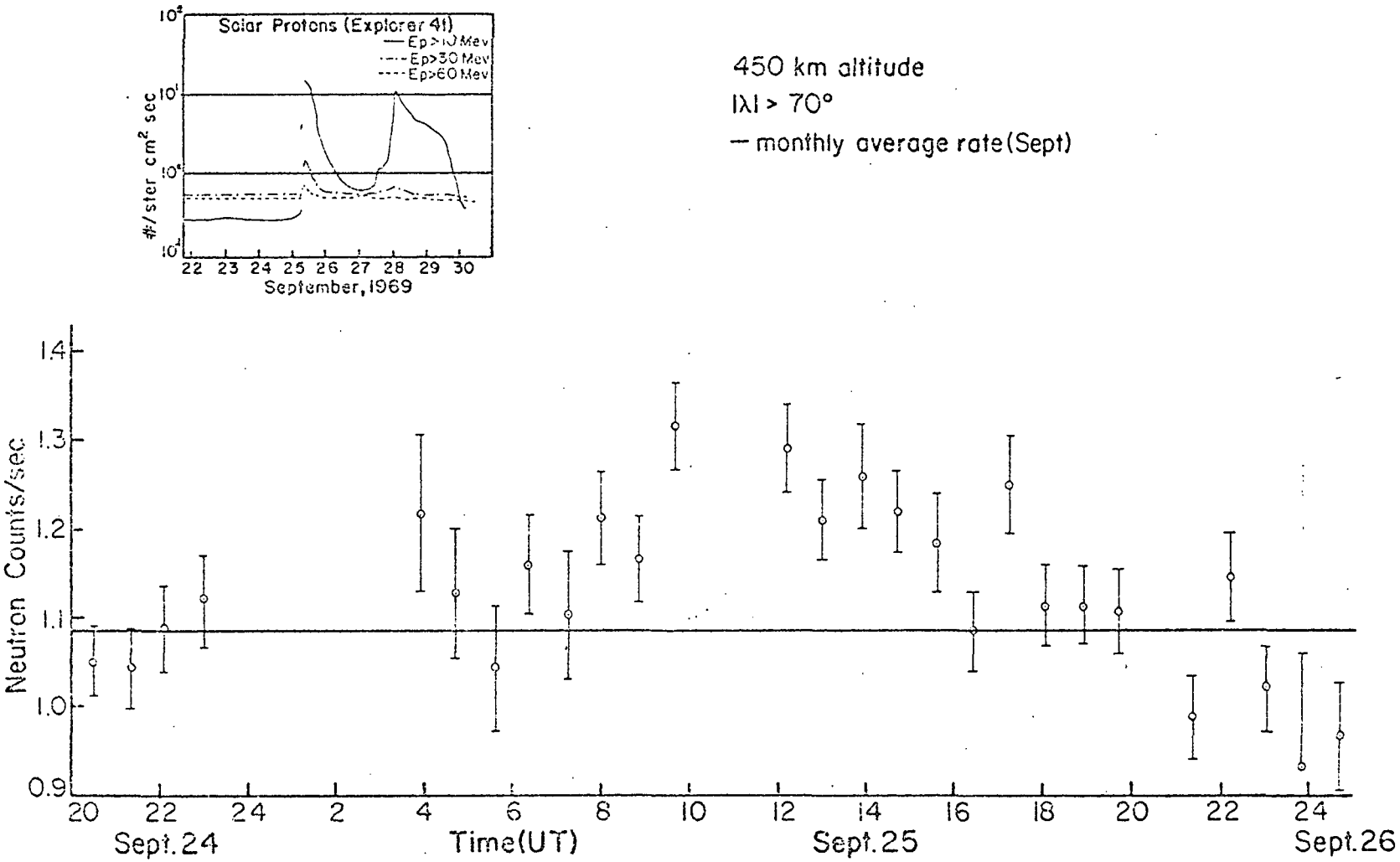
Solar Protons (Explorer 41)
Ep>10 Mev
Ep>30 Mev
Ep>60 Mev
#/ster cm² sec
September, 1969
450 km altitude
|λ| > 70°
— monthly average rate (Sept)
Neutron Counts/sec
Time(UT)
Sept. 24
Sept. 25
Sept. 26

Figure 1

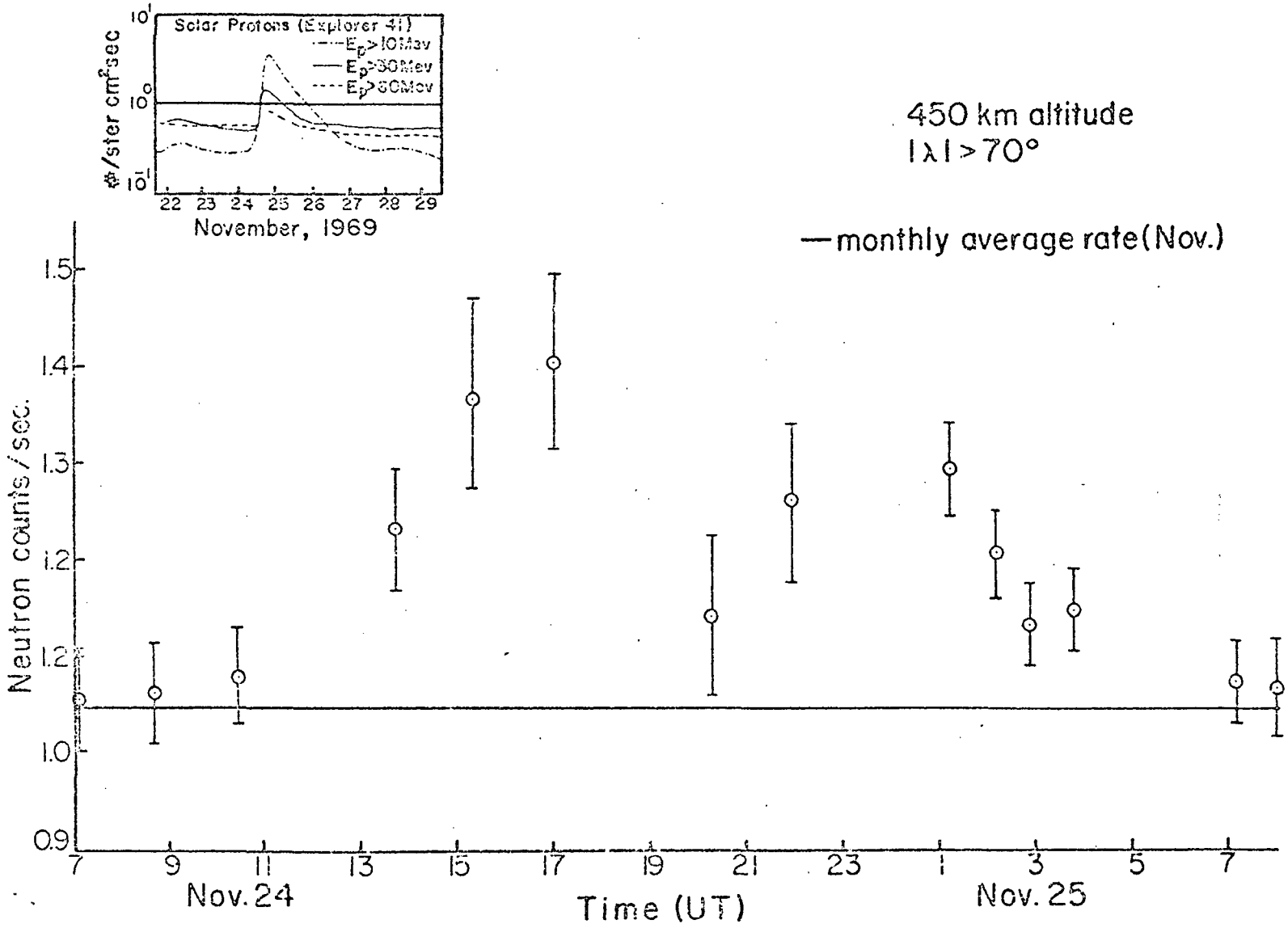
Solar Protons (Explorer 41)
E_p>10Mev
E_p>30Mev
E_p>60Mev
#/ster cm²sec
November, 1969
450 km altitude
|λ|>70°
—monthly average rate(Nov.)
Neutron counts/sec.
Nov. 24
Time (UT)
Nov. 25

Figure 2

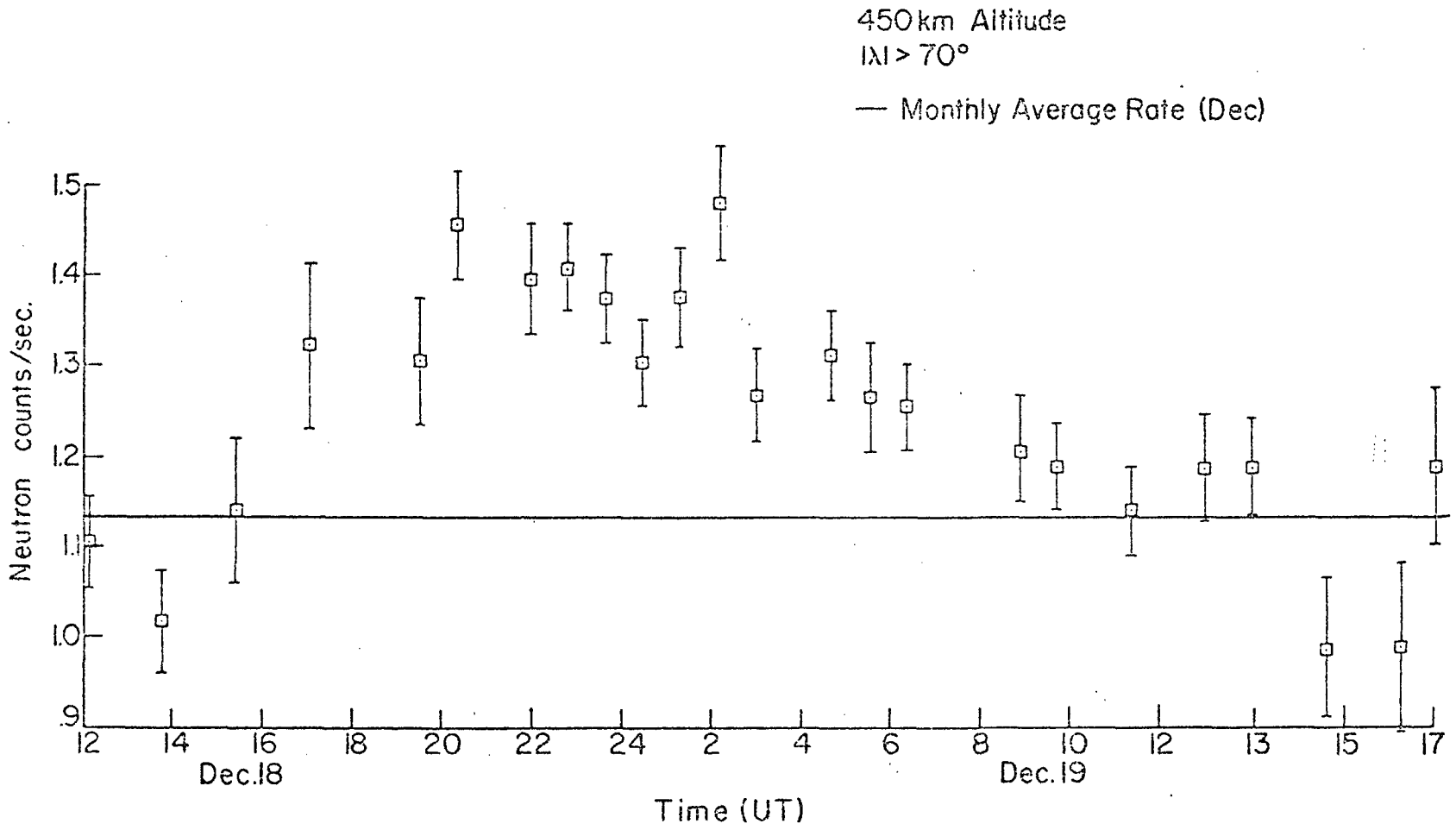
450 km Altitude
|λ| > 70°
— Monthly Average Rate (Dec)
Neutron counts/sec.
1.5
1.4
1.3
1.2
1.1
1.0
.9
12
14
16
18
20
22
24
2
4
6
8
10
12
13
15
17
Dec.18
Dec.19
Time (UT)

Figure 3

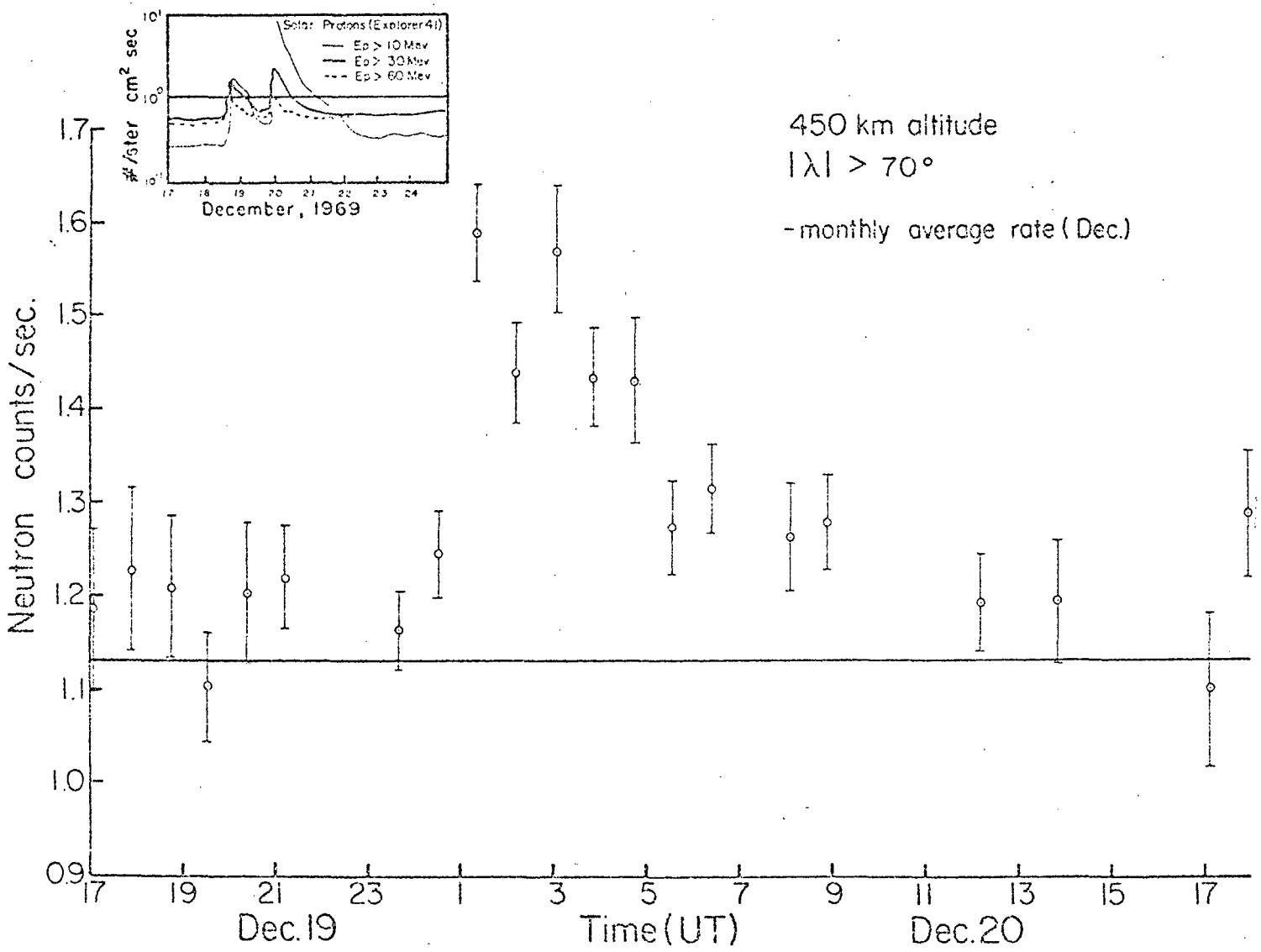
Solar Protons (Explorer 41)
Ep > 10 Mev
Ep > 30 Mev
Ep > 60 Mev
#/ster cm² sec
December, 1969
450 km altitude
|λ| > 70°
- monthly average rate (Dec.)
Neutron counts/sec.
1.7
1.6
1.5
1.4
1.3
1.2
1.1
1.0
0.9
17 19 21 23 1 3 5 7 9 11 13 15 17
Dec.19
Time (UT)
Dec.20

Figure 4

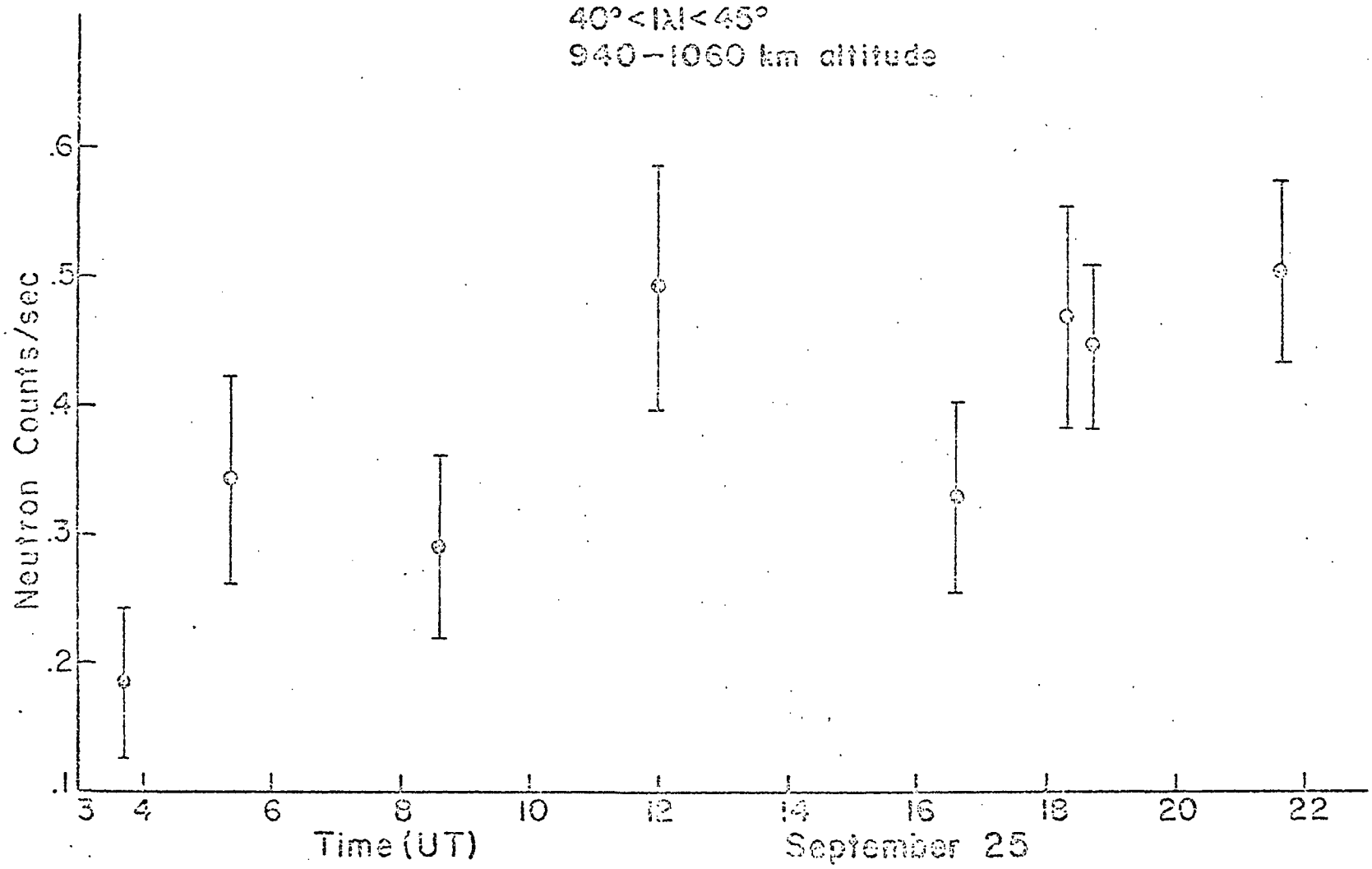
40°<|λ|<45°
940–1060 km altitude
Neutron Counts/sec
.1
.2
.3
.4
.5
.6
3
4
6
8
10
12
14
16
18
20
22
Time (UT)
September 25

Figure 5a

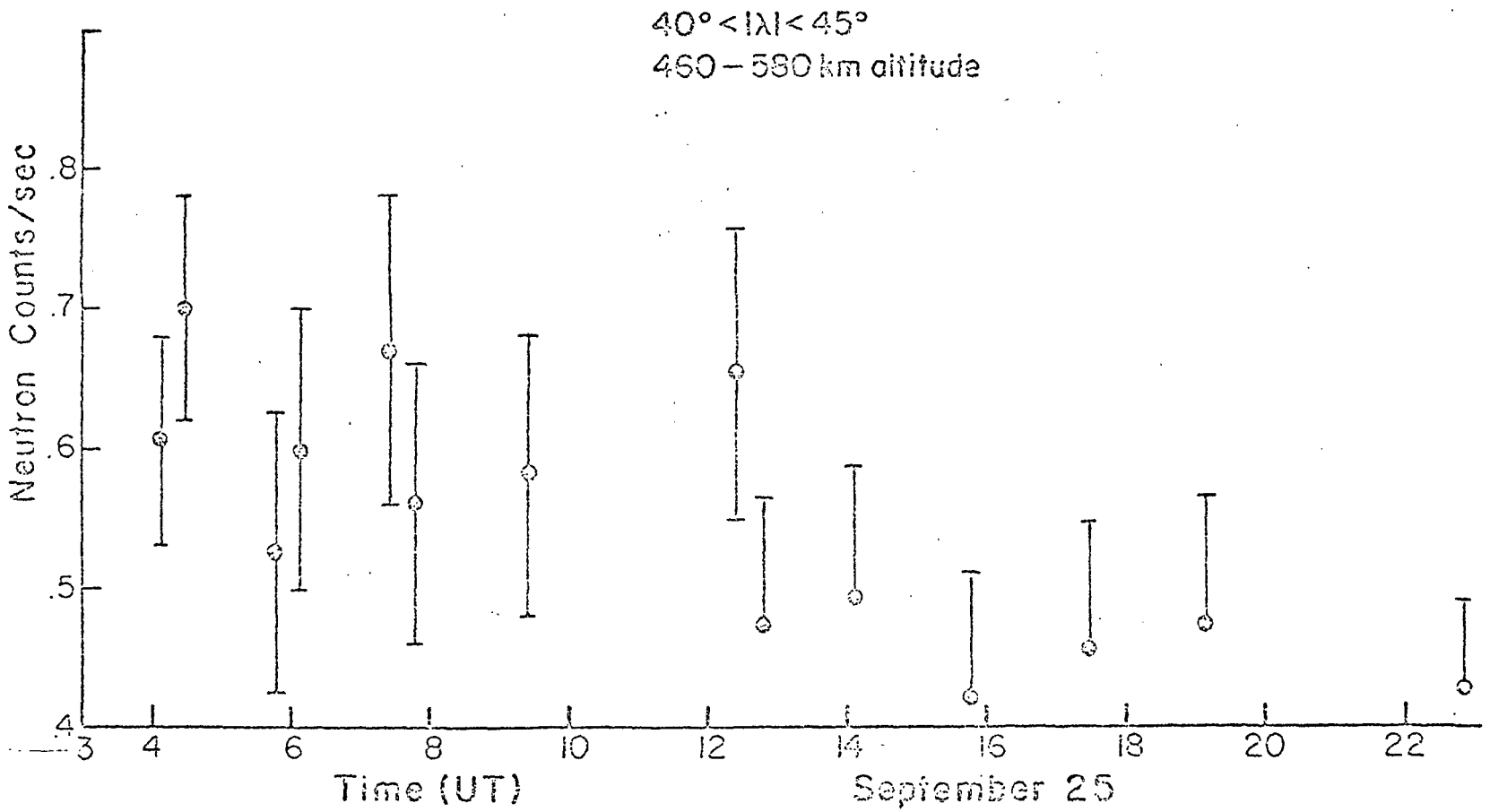
40° < |λ| < 45°
460 – 580 km altitude
Neutron Counts/sec
.8
.7
.6
.5
.4
3
4
6
8
10
12
14
16
18
20
22
Time (UT)
September 25

Figure 5b

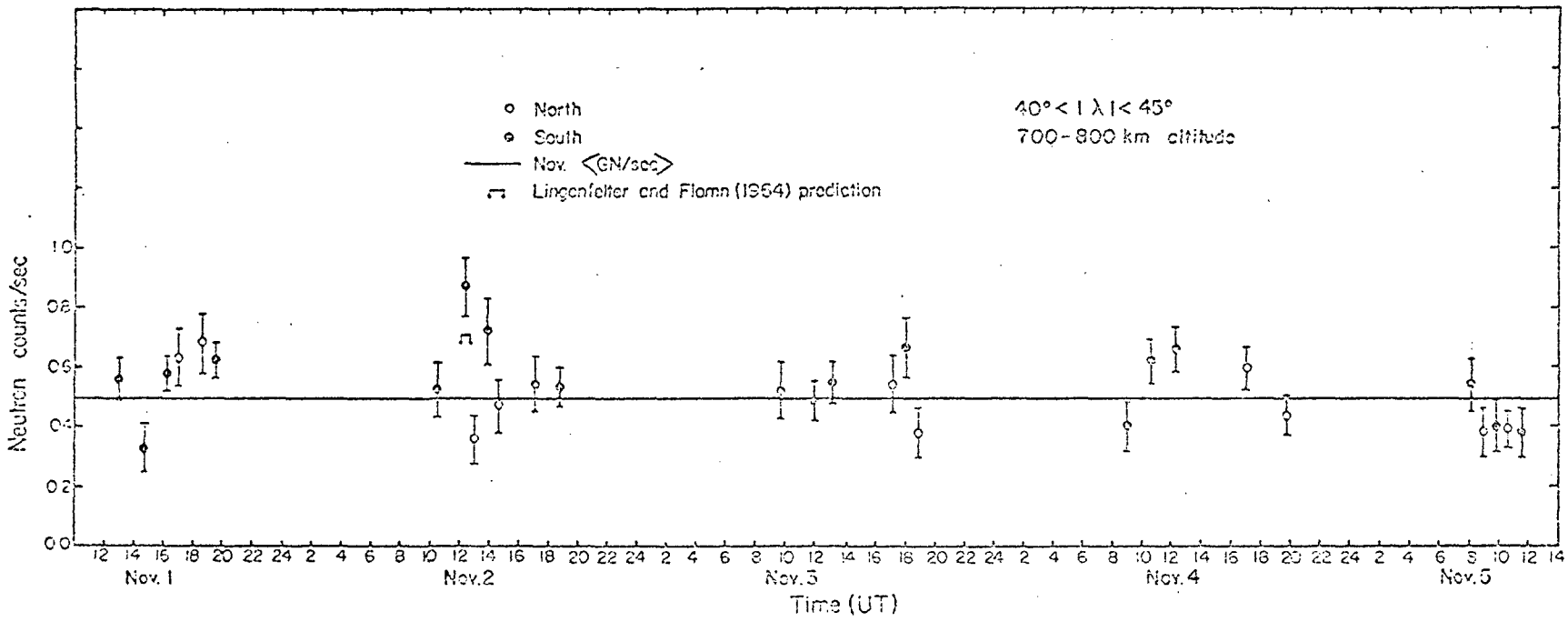
North
South
Nov. ⟨GN/sec⟩
Lingenfelter and Flamm (1964) prediction
40° < | λ | < 45°
700 - 800 km altitude
Neutron counts/sec
0.0
0.2
0.4
0.6
0.8
1.0
12 14 16 18 20 22 24 2 4 6 8 10 12 14 16 18 20 22 24 2 4 6 8 10 12 14 16 18 20 22 24 2 4 6 8 10 12 14 16 18 20 22 24 2 4 6 8 10 12 14
Nov. 1
Nov. 2
Nov. 3
Nov. 4
Nov. 5
Time (UT)

Figure 6

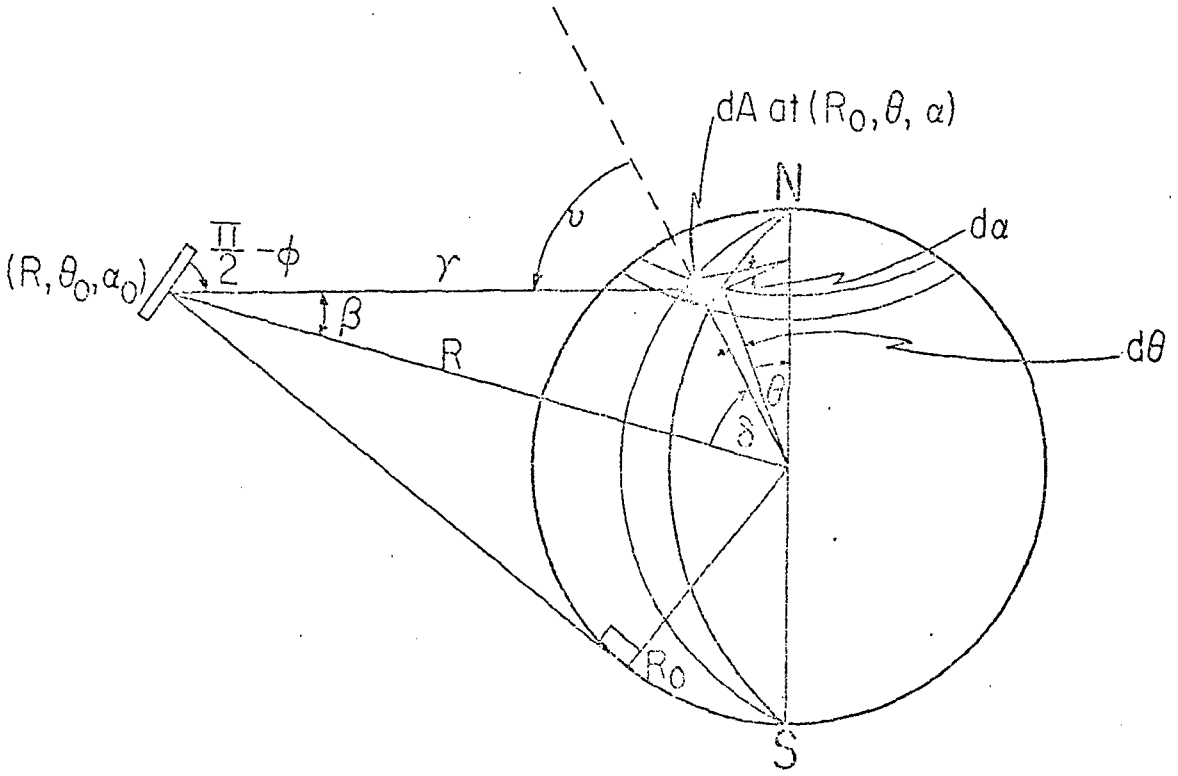

The geometry of the altitude variation of the neutron counting rate.

Figure 7

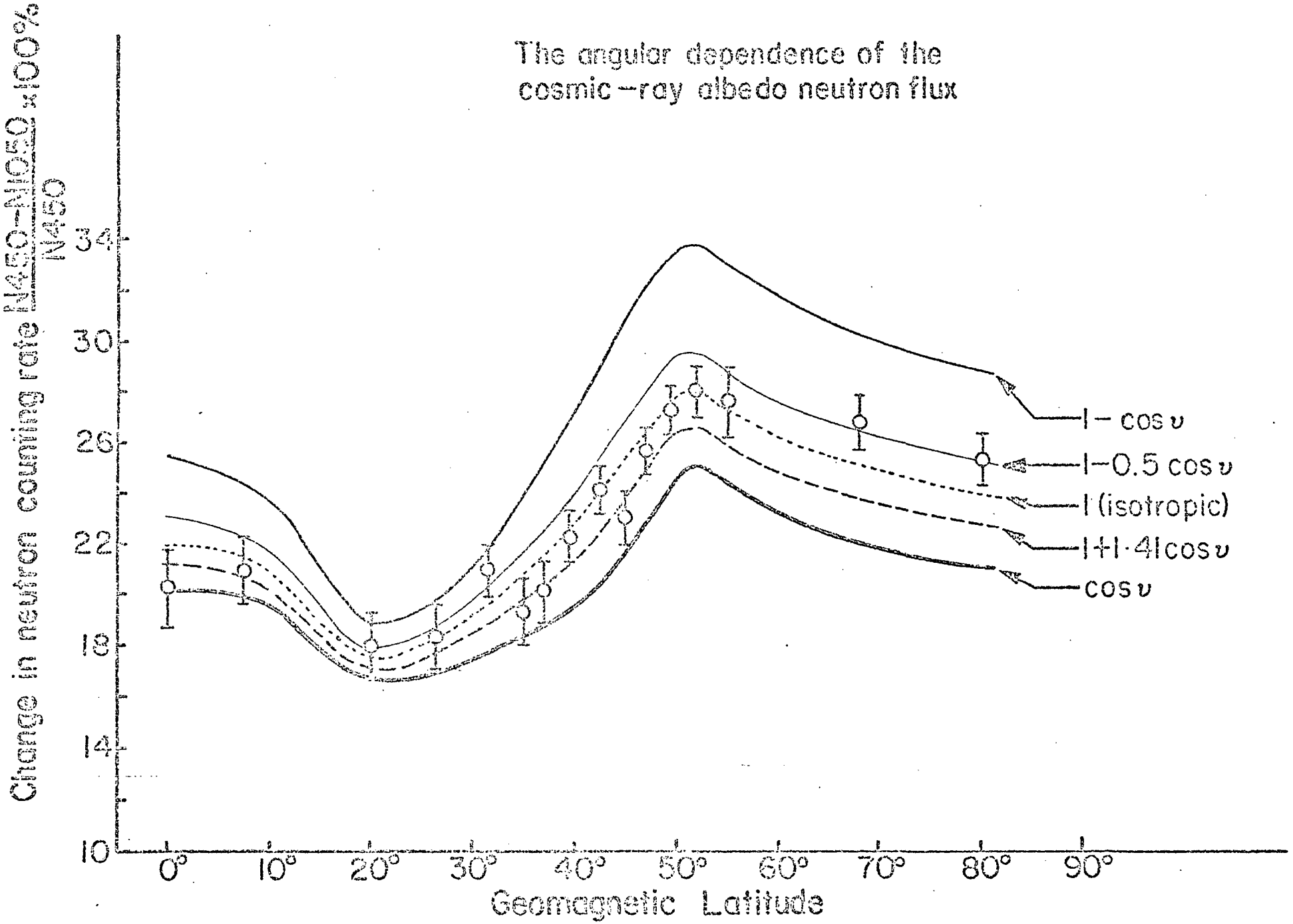
The angular dependence of the
cosmic-ray albedo neutron flux
Change in neutron counting rate (N450-N050)/N450 ×100%
34
30
26
22
18
14
10
0°
10°
20°
30°
40°
50°
60°
70°
80°
90°
Geomagnetic Latitude
1 - cos υ
1-0.5 cos υ
1 (isotropic)
1+1·4 cos υ
cos υ

Figure 8

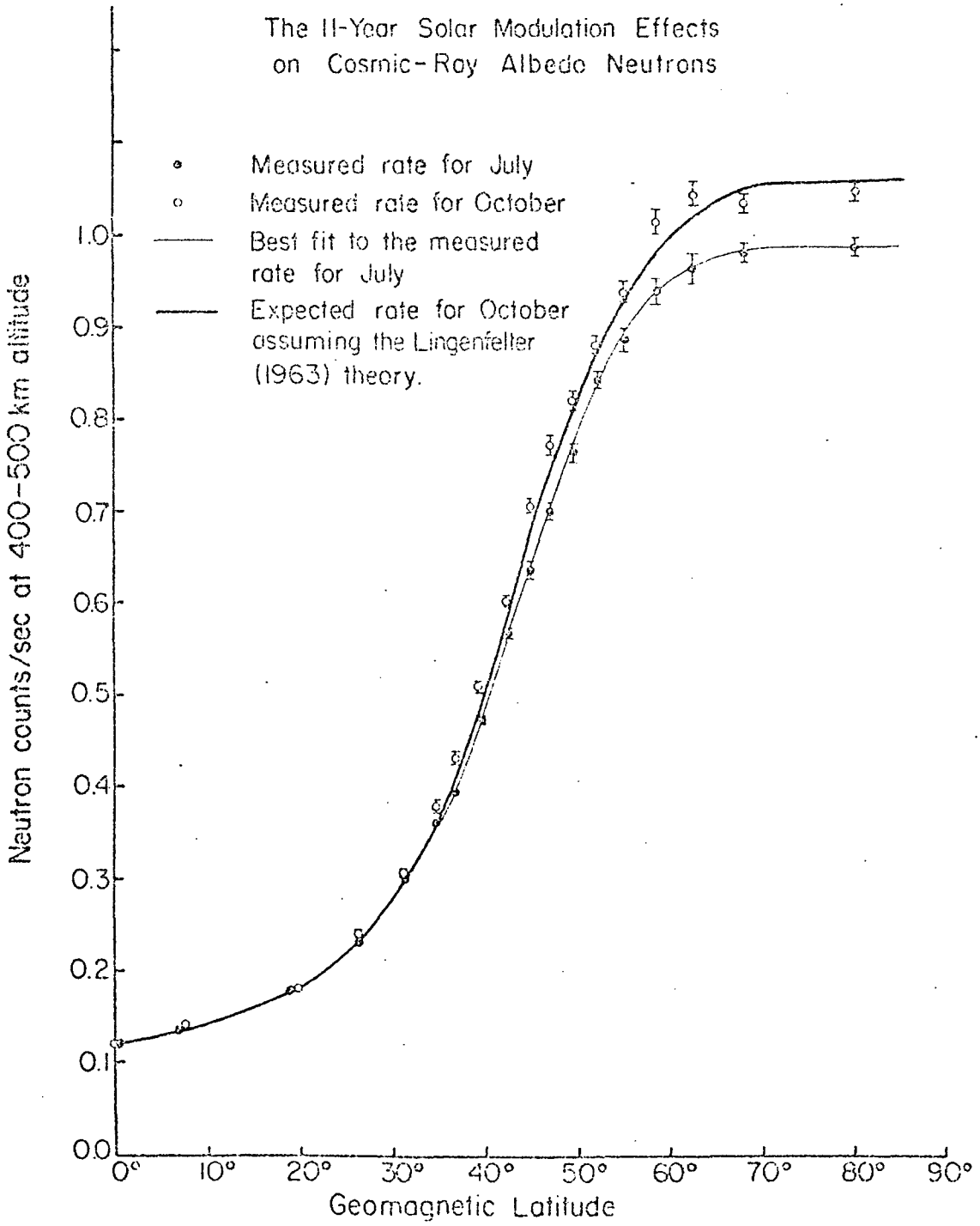
The 11-Year Solar Modulation Effects
on Cosmic-Ray Albedo Neutrons
Measured rate for July
Measured rate for October
Best fit to the measured rate for July
Expected rate for October assuming the Lingenfelter (1963) theory.
Neutron counts/sec at 400-500 km altitude
0.0
0.1
0.2
0.3
0.4
0.5
0.6
0.7
0.8
0.9
1.0
0°
10°
20°
30°
40°
50°
60°
70°
80°
90°
Geomagnetic Latitude

Figure 9

COSMIC RAY NEUTRON MONITOR FOR OGO-F

BY

J. A. LOCKWOOD, E. L. CHUPP, AND R. W. JENKINS

Reprinted from IEEE TRANSACTIONS
ON *GEOSCIENCE ELECTRONICS*
Volume GE-7, Number 2, April, 1969
pp. 88-93

tion of phoswiching and pulse-shape discrimination (PSD) to separate neutrons from charged particles and gamma rays. The neutron energy spectrum itself was not determined and the results must be extrapolated to the top of the atmosphere to evaluate the neutron leakage flux. The high-energy spectrum in the range $12 < E_n < 100$ MeV at atmospheric depths of 9 g·cm^{-2} and geomagnetic latitude 42°N has been measured by Zych and Frye [4]. They observe that the proton recoil spectrum was found to depend upon $E^{-3.3}$. This proton spectrum is interpreted as due to a highly anisotropic, high-energy neutron flux near the top of the atmosphere. The extrapolated flux value at 0 g·cm^2 is 0.11 n/cm^2 seconds, an order of magnitude greater than Lingenfelter [5] calculates. The most precise fast-neutron measurements ($3 < E_n < 20$ MeV) have been made recently by St. Onge [6] with a proton recoil scintillator utilizing a separate charged-particle rejection scheme with a multiparameter display system for the PSD which separates gamma rays from neutrons. Unfortunately, data, so far, have been obtained only at the Pfotzer maximum. These results indicate that the neutron spectrum depends upon $E^{-\alpha}$, where α is $\simeq 4$ at $E = 3.0$ and $\alpha \simeq 1.5$ at 15 MeV. Also, a much larger ratio of gamma-rays to neutrons was observed, which suggests that the experimental difficulties are greater than anticipated. The neutron leakage flux in the energy interval 0–15 MeV has been measured recently by rocket flights of moderated He^3 neutron detectors at several latitudes [7]. For latitudes of 0° and 70° the integral fluxes were 0.08 ± 0.02 and 0.80 ± 0.10 n/cm^2·s, respectively. These results are in better agreement with the neutron leakage fluxes calculated by Lingenfelter [5] and Newkirk [8] than earlier experimental values, although the latitude dependence of the integral flux is not so large as predicted by Lingenfelter [5].

From this brief survey of the current knowledge about the neutron flux and energy spectrum both within and outside the atmosphere, we can see that many unsolved problems exist. First, within the atmosphere (at ~ 5 g·cm^{-2}) the neutron energy spectrum in the range $1 < E_n < 50$ MeV has not been precisely determined. Very few attempts have been made to determine the directionality of the fast-neutron flux. Second, above the atmosphere there is disagreement between theory and experiment about the magnitude of the total neutron intensity. The energy spectrum in the 1–50 MeV range has not been precisely determined. The neutron intensity dependence upon distance from the earth is known only approximately [9] and definitive measurements have not been made of the angular distribution of the neutrons diffusing from the atmosphere. Both the theoretical and experimental values for the neutron leakage flux have been used to evaluate the contributions which are made to the trapped radiation from the decay of these neutrons [10], [11]. The results of such calculations indicate: 1) solar neutrons and solar protons make an insignificant contribution; 2) the flux of trapped protons with $E < 20$ MeV cannot be accounted for by the neutron decay mechanism; and 3) the magnitude of the contribution from this source to the trapped protons with $E > 20$ MeV is unresolved, the results from the theoretical calculations disagree with those expected from the measured leakage flux by more than an order of magnitude. Measurements of the fast neutron flux and energy spectrum should help resolve these differences.

The experiment which we have designed can determine the latitude dependence of the integral neutron flux in the energy range 10^{-8}–15 MeV, as well as the longitude and altitude dependence. However, since the neutron sensor has an omni-directional response, no information on the anisotropy of the neutron flux can be acquired. The neutron energy spectrum in the interval 1–10 MeV can be deduced from the plastic scintillator used as a proton recoil detector in coincidence with the He^3 counter.

Neutron Sensor

A. Description

Since the neutron intensity is measured in a background of energetic charged particles, which can produce neutrons in the sensor, it must include a scheme to reject neutrons associated with charged-particle events. Also, the sensor must clearly separate neutrons from gamma rays. The best estimates indicate that the integrated neutron leakage fluxes at latitudes of 90° and 0° are < 1.0 and < 0.08 n/cm^2·s, respectively. Consequently, the sensor must have a reasonable efficiency for neutron detection and a low background counting rate.

The neutron sensor chosen for this mission is similar to the types flown on three USAF Discoverer satellites [12] and, recently, on a series of rocket flights [7]. A He^3 proportional counter, which detects neutrons indirectly through the nuclear reaction He^3 (n, p)H^3, is surrounded by a plastic scintillator as shown in Fig. 1. The plastic scintillator acts both as a moderator for fast neutrons and a detector of proton and carbon recoils produced in the slowing down of the neutrons. This represents a unique application of a scintillator-type neutron detector. Hence, this moderated He^3 counter can be used

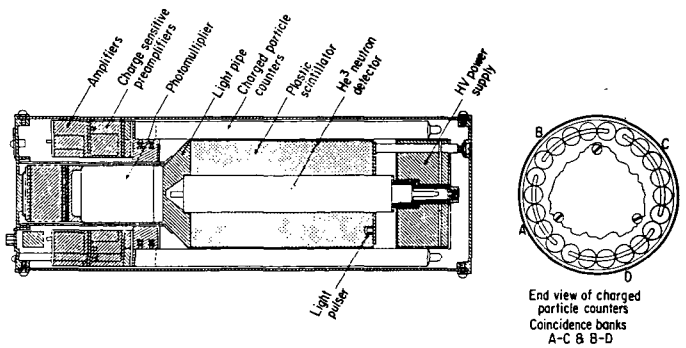

Fig. 1. Neutron sensor.

tem using laboratory beams of energy 2.4 and 14 MeV. In the actual flight unit the same definition of the pulse-height distribution cannot be obtained because only four pulse-height channels are used. These four channels are determined by the integral discrimination levels A–E inclusive. Crude measurements indicate that the efficiencies for the four channels (A–B, B–C, C–D, D–E) with the integral discriminators set as in Fig. 2 are 0.03, 0.08, 0.14, and 0.05 cm², respectively, at 2.4 MeV and are 0.013, 0.011, 0.017 and 0.030 cm², respectively, at 14 MeV.

In order to use the data in these four channels to determine the unknown energy spectrum the efficiencies of these channels for neutrons of many different energies from 1 to 20 MeV must be determined. The counting rate for each channel may be written

$$C_j = \sum_{i=i}^{n} P_j(E_i)N(E_i)\Delta_i E, \quad \text{for } j = 1, 2, 3, 4 \qquad (1)$$

where j designates the channel number, $P_j(E_i)$ = the efficiency of channel j for neutrons of energy E_i, and $\Delta_i E$ = energy interval, and $N(E_i)$ = the unknown neutron energy spectrum. This assumes that the efficiencies $P_j(E_i)$ have been determined for a large number of different neutron energies so that over $\Delta_i E$ the values of $P_j(E_i)$ and $N(E)$ are essentially constant. If we assume that the energy spectrum is of the form $N(E) = AE^{-\gamma}$ then (1) becomes

$$C_j = A \sum_{i=i}^{n} P_j(E_i)(E_i^{-\gamma})\Delta_i E \quad \text{for } j = 1, 2, 3, 4. \qquad (2)$$

We know C_j from the experimental data and $P_j(E_i)$ and $\Delta_i E$ from the calibrations. In order to find A and γ we can assume values for them and calculate the expected values of C_j. A comparison between the calculated and measured C_j will determine what values, if any, of the assumed neutron spectrum parameters, A and γ, are reasonable fits to the data. Other functional forms for the neutron spectrum may also be attempted in order to determine which form is best capable of fitting the data.

C. Summary of Sensor Properties

The specifications for the neutron sensor are as follows: weight = 5.7 lb (2.58 kg); length = $12\frac{3}{8}$ inches. (0.314 meter); diameter = $4\frac{3}{8}$ inches (0.111 meter); power requirements 4.5 watts. The estimated efficiency for the neutron leakage spectra is about 1.8 cm². In the fast mode the efficiency at any energy value in the interval 1–10 MeV is about 10 percent of the efficiency in the total mode. In addition to the leakage flux measurements, the energy spectrum 1–10 MeV can be evaluated from the other simultaneous mode of operation. The sensor has excellent discrimination against gamma rays and a low background counting rate.

D. Electronics System

In discussing the electronics system for the experiment, we will consider first that section pertaining to the charged-particle monitoring, then the section of the system related to the total neutron flux, and finally those parts dealing with the fast-neutron measurements. Since the experiment required more data output than could be handled with only the three main frame words provided us on the spacecraft, an internal subcommutator sequence was incorporated within the experiment. In Fig. 3, only the experiment words are indicated with no reference to the subcommutator sequence.

Referring to Fig. 3, we see that both coincidence rates A–C and B–D and the total counting rate (A+B+C+D) of the charged-particle guard counters is read out on separate experiment words designated words 2, 3, and 5, respectively. Since extremely high counting rates ($>10^4$ per second) are expected when the spacecraft passes near and through the radiation belts, a logarithmic counting rate meter is provided (spacecraft subcommutator analog word 86). Since it is expected that the charged-particle rates, both total and coincidence (as well as the total neutron rate) will vary from 1 to 10^4 per second, a logarithmic prescaling system was incorporated into these channels (experiment words 2, 3, and 5). If the counting rate is low so that less than 64 events are stored between readouts, then the number of events accumulated equals the word reading. But if, for example, the word is greater than 63 but less than 128, the number of events equals 65+2× (word reading 64). Thus, the maximum information which can be stored is then 2756 for experiment word 5 (9-bit word) and 708 for experiment words 1, 2, and 3 (8-bit words).

The neutron counter output is directly fed into experiment word 1, designated the ungated or total counting rate. This rate is due to neutrons incident from outside

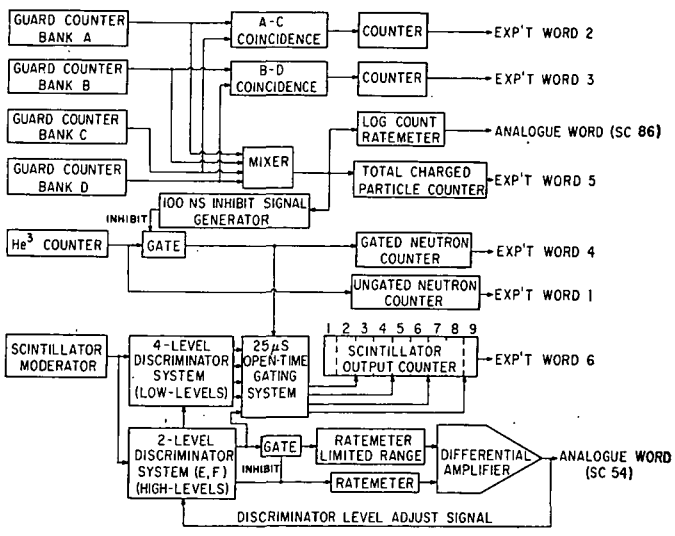

Fig. 3. Schematic diagram of electronics system.

Acknowledgment

In the initial testing phases J. Haussler was most helpful. Miss L. Townsend assisted in calibration of the prototype and flight units at the University of New Hampshire. Marshall Laboratories, Inc., designed the electronics system and constructed both units. We are grateful to G. Spellman and R. Hill for their conscientious efforts in the construction and flight qualification of the system.

References

[1] S. F. Singer, "Trapped albedo theory of the radiation belt," *Phys. Rev. Letters*, vol. 1, p. 181, 1958.
[2] R. C. Haymes, "Terrestrial and solar neutrons," *Rev. Geophys.*, vol. 3, p. 345, 1965.
[3] S. S. Holt, R. B. Mendell, and S. A. Korff, "Fast neutron latitude variations in the atmosphere at solar minimum," *J. Geophys. Res.*, vol. 71, p. 5109, 1966.
[4] A. D. Zych and G. M. Frye, Jr., "High-energy albedo neutrons near the top of the atmosphere," *Am. Phys. Soc. Bull.*, vol. 13, p. 1434, 1968.
[5] R. E. Lingenfelter, "The cosmic-ray neutron leakage flux," *J. Geophys. Res.*, vol. 68, p. 5633, 1963.
[6] R. N. St. Onge, "The energy spectrum and flux of fast neutrons in the atomosphere," Ph. D. dissertation, University of New Hampshire, Durham, 1969.
[7] J. A. Lockwood and L. A. Friling, "Cosmic-ray neutron flux measurements above the atmosphere," *J. Geophy. Res.*, vol. 73, p. 6649, 1968.
[8] L. I. Newkirk, "Calculation of the low-energy neutron flux in the atmosphere by the S_n method," *J. Geophys. Res.*, vol. 68, p. 1825, 1963.
[9] W. N. Hess and A. J. Starnes, "Measurement of the neutron flux in space," *Phys. Rev. Letters*, vol. 5, no. 2, p. 48, 1960.
[10] A. J. Dragt, M. M. Austin, and R. S. White, "Cosmic-ray and solar proton albedo neutron decay injection," *J. Geophys. Res.*, vol. 71, p. 1293, 1966.
[11] W. N. Hess and J. Killeen, "Spatial distribution of protons from neutron decay trapped by the geomagnetic field," *J. Geophys. Res.*, vol. 71, p. 2799, 1966.
[12] J. H. Trainor and J. A. Lockwood, "Neutron albedo measurements on polar orbiting satellites," *J. Geophys. Res.*, vol. 69, p. 3115, 1964.

Journal of
GEOPHYSICAL RESEARCH
Space Physics

VOLUME 75 August 1, 1970 No. 22

Latitude and Altitude Dependence of the Cosmic Ray Albedo Neutron Flux

R. W. JENKINS, J. A. LOCKWOOD, S. O. IFEDILI, AND E. L. CHUPP

Space Science Center and Physics Department
University of New Hampshire, Durham 03824

Preliminary measurements of the cosmic ray albedo neutron flux above 400 km are reported for the period June 7 to 17, 1969. The measurements were made with a detector on board the Ogo 6 satellite that responds primarily to neutrons in the energy range 10^4 to 10^6 ev. The latitude variation of the counting rate was found to be 7.4/1 between 90° and 0°, similar to that predicted by Lingenfelter (1963). The neutron counting rate near the poles was found to decrease by 26 ± 5% between 450 and 950 km altitude, corresponding to a $R^{-4.8 \pm 0.9}$ dependence, where R is the distance from the center of the earth. This large altitude dependence excludes any angular distributions of neutron flux at the top of the atmosphere that are more peaked toward the vertical than cos θ (where θ is the angle from the vertical), but it is not in disagreement with an isotropic neutron flux. The total neutron leakage flux found by assuming isotropy was about 0.7 times that predicted by Lingenfelter (1963). The neutron leakage flux values obtained from the Ogo 6 experiment agree with those estimated from other experiments with a similar neutron energy response, if the same angular distribution is used. Estimates of the total neutron leakage flux, deduced from experiments responsive only to neutrons above 1 Mev by using the Lingenfelter (1963) and Newkirk (1963) energy spectra of leakage neutrons, show agreement with the lower energy results when the Newkirk spectrum is used but are up to twice as great as the lower energy results when the Lingenfelter spectrum is applied.

In this paper we present preliminary measurements of the cosmic ray albedo neutron flux in the energy range 10^5–10^7 ev from a neutron detector on board the orbiting geophysical observatory Ogo 6, a polar-orbiting satellite with altitudes between 400 and 1100 km. From these measurements, the latitude and altitude dependence of the neutron flux for the initial turn-on period, June 7–17, 1969, have been determined. The June 7–17 period is typical in terms of the solar and geomagnetic activity present during this phase of the current solar cycle, with no exceptional solar flare events reported [*Solar Geophysical Data*, 1969].

DETECTOR DESCRIPTION

The components of the neutron sensor and its orientation with respect to the spacecraft and the earth are depicted in Figure 1. The sensor was located approximately 5 meters out on the EP-5 boom to minimize the background of neutrons that are produced in the main body of the spacecraft by the cosmic radiation.

The detector consists of a proportional counter filled with He^3, sensitive primarily to thermal neutrons through the reaction $He^3(n, p)H^3$,

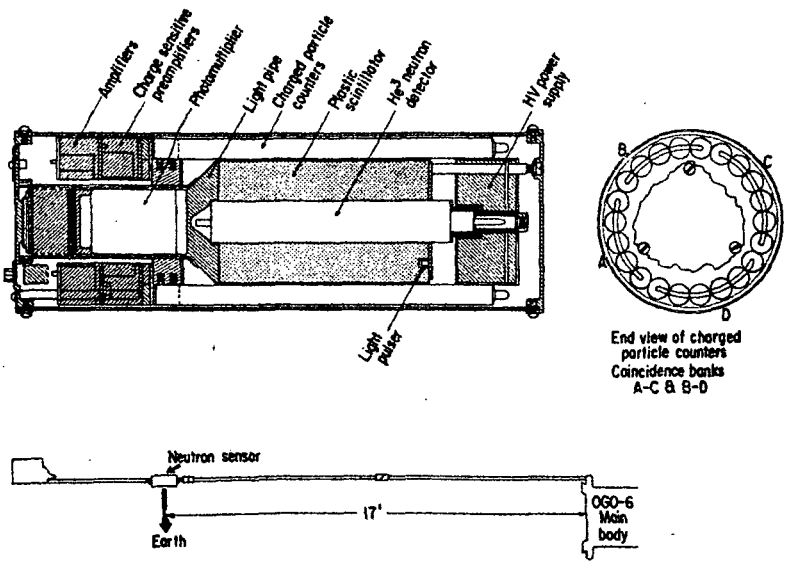

Fig. 1. Neutron sensor arrangement and orientation on Ogo 6 spacecraft.

surrounded by a plastic scintillator and a ring of charged-particle guard counters. The plastic scintillator serves two functions. First, it acts as a moderator for fast neutrons, by slowing them down to energies where they can be detected more efficiently by the He^3 counter. Second, it is used to measure the neutron energy in the range 1–10 Mev. The neutron energy distribution is deduced from the pulse height distribution of scintillation events followed within 25 microseconds by a He^3 counter event. The ring of charged-particle guard counters acts as an anti-coincidence shield against cosmic ray nuclei that can produce neutrons in the material adjacent to the He^3 counter. As shown in Figure 1, the charged-particle counters are arranged in four banks, *A*, *B*, *C*, and *D*. The signals from the four banks are summed and are also put into the coincidence pairs *A-C* and *B-D*. A more complete description of the sensors with associated electronics has been published [*Lockwood et al.*, 1969].

The following data are acquired by the neutron sensor: (*a*) the total number of events in the He^3 proportional counter (N_T); (*b*) the number of events in the He^3 counter not associated with events in the charged-particle guard counters (N_G); (*c*) the number of scintillator events associated with events in category (*b*), stored in a 4-channel pulse-height analyzer; (*d*) the number of events in the charged-particle guard counter (N_{ABCD}); (*e*) the numbers of coincidences between the two pairs of charged-particle counter banks (N_{AC}, N_{BD}). In this paper we are reporting total neutron measurements and concern ourselves primarily with the quantities N_T, N_G, N_{ABCD}, N_{AC}, and N_{BD}.

Detector Efficiency

The neutron detector was calibrated as a function of neutron energy by exposing it to known neutron fluxes from both Am^{241}-Li, Am^{241}-Be, and Am^{241}-mock fission radioactive sources and monoenergetic neutrons ranging from 5 kev to 20 Mev produced in the reactions $Sc^{45}(p, n)Ti^{45}$, $H^3(p, n)He^3$, $H^3(d, n)He^4$, and $H^2(d, n)He^3$, by using the 5.5-Mev Van der Graaf accelerator at the Oak Ridge National Laboratories. The neutron detector efficiency for events in the He^3 counter, as a function of energy for an isotropic neutron flux, is shown in Figure 2.

The measurements of detector efficiency for neutrons from the radioactive sources provided a check on the absolute efficiencies deduced from the monoenergetic measurements. From the observed variation of the monoenergetic neutron efficiency with energy and the neutron energy distributions for the Am^{241}-Be, Am^{241}-Li, and Am^{241}-mock fission neutron sources [*Han-*

sen, 1960; *Geiger and Hargrove*, 1964], the efficiencies expected for these radioactive sources were calculated. The measured efficiencies for the sources were then plotted in Figure 2, at neutron energies for which the monoenergetic curve gives the calculated efficiencies. It can be seen from Figure 2 that the efficiencies measured for the radioactive sources agree with those obtained from the monoenergetic neutron measurements.

To extrapolate the neutron efficiency for the detector to lower energies, we have used the measurements of *Tatsuta et al.* [1965] with cylindrical paraffin-moderated BF_3 counters. The solid curve in Figure 2 is the expected efficiency as a function of energy based on their measurements. To adapt the results of Tatsuta's measurements to the Ogo 6 detector, we interpolated his results to derive a neutron efficiency versus energy curve for an amount of hydrogen per unit length of moderator equal to that of the Ogo 6 detector. The neutron efficiency curve thus derived was normalized to the measured values obtained in the energy range 5 kev to 2.5 Mev. It is evident from Figure 2 that the deduced curve agrees with the energy dependence of efficiency found from 0.1 to 2.5 Mev. At energies above 2.5 Mev, the efficiencies measured here are greater than those deduced from Tatsuta's measurements, probably due to the moderating effects of inelastic neutron collisions with the relatively greater number of carbon nuclei surrounding the Ogo 6 detector.

To derive a mean efficiency for the albedo neutron flux, the efficiency curve (Figure 2) was folded into the albedo neutron energy spectrum predicted for the present level of solar activity by *Lingenfelter* [1963]. The mean efficiency was also derived by using the calculated neutron energy spectrum of *Newkirk* [1963]. The mean efficiencies obtained for an isotropic neutron flux and the anticipated contributions from the various neutron energy ranges to the counting rate of our detector are listed in Table 1. From this table we see that the largest fraction of the counting rate is from neutrons in the energy range 10^4 to 10^6 ev for both energy spectra. The mean efficiencies for the two assumed spectra of leakage neutrons differ by 22%.

The variation of the detector efficiency with the incident angle of the neutron flux was determined by using neutrons from the Am^{241}-Li source ($\langle En \rangle$ = 390 kev) and the reaction $H^3(d, n)He^4$ (En = 14 Mev). The angular dependence of relative response shown in Figure 3 is energy independent. The measured angular response curve (Figure 3) was used to convert the measurements taken with monoenergetic neutrons incident perpendicular to the axis of symmetry of the detector into the absolute efficiencies for isotropically incident neutron fluxes plotted in Figure 2. Because the re-

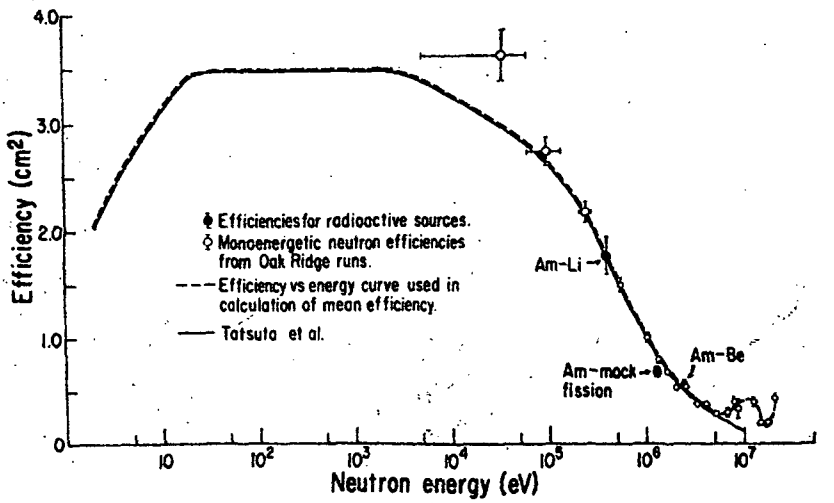

Fig. 2. Response of detector for isotropic neutron fluxes as a function of energy.

TABLE 1. Predicted Contributions to the Counting Rate of the Ogo 6 Neutron Detector*

Neutron Energy, ev	Percentage of Neutron Counting Rate *Lingenfelter* [1963] Spectrum	*Newkirk* [1963] Spectrum
$<10^1$	2.3	4.7
10^1–10^2	4.2	6.0
10^2–10^3	6.7	8.0
10^3–10^4	10.8	13.4
10^4–10^5	16.3	15.2
10^5–10^6	47.4	33.8
10^6–10^7	11.5	16.3
$>10^7$	0.8	2.6
Mean detector efficiency for isotropic flux, cm^2	1.59 ± 0.16	1.30 ± 0.13

* From various energy ranges of leakage neutrons for the *Lingenfelter* [1963] and the *Newkirk* [1963] energy spectra for neutron leakage flux.

sponse of the detector depends upon the direction of the incident neutrons, the neutron flux in space derived from the observed counting rate will depend on the assumed angular distribution of neutrons in the vicinity of the detector. The effect is small for the orientation of the neutron detector on the Ogo 6 spacecraft, however, because all physically acceptable angular distributions are cylindrically symmetrical about the vertical. The calculated response for different angular distributions varies by less than 15% from that expected for an isotropic neutron flux.

Correction for Locally Produced Neutrons

The total neutron counting rate N_T of the Ogo 6 detector arises from three sources: (1) neutrons external to the spacecraft, i.e., not produced in the spacecraft or detector; (2) neutrons produced in the detector by charged particles seen by the guard counters; and (3) neutrons produced in the spacecraft and detector by charged particles not seen in the guard counter. The gated neutron counting rate, N_G, arises from neutrons in categories (1) and (3). The counting rate due to the neutrons external to the experiment (N_G') was estimated by using the increase in neutron counting rate when the Ogo 6 satellite passed through the South Atlantic magnetic anomaly. Protons with energies of the order of 100 Mev that were present in the anomaly gave rise to enhanced local neutron production. From these observations the ratio of counts from locally produced neutrons in category (3) to counts from category (2) neutrons was obtained. During other times, the gated neutron rate N_G could be corrected for neutrons in category (3) by noting the count rate due to neutrons in category (2), $(N_T - N_G)$, and by using the ratio found in the anomaly. We found that the counting rates due to locally produced neutrons in categories (2) and (3) were approximately 35% and 12% of the total neutron counting rate N_T, respectively.

Results

The gated neutron data corrected for locally produced neutrons (N_G') were sorted according to geomagnetic latitude and altitude into 5° by 100-km bins. Neutron counting rates corresponding to charged particle rates in excess of 2.5 times the minimum values for that latitude were excluded from this analysis.

Latitude and altitude dependence. In Figure 4 the neutron rates N_G' for the 400- to 500-km altitude region are plotted as a function of geomagnetic latitude. The latitude dependence of counting rate from the poles to the equator is found to be 7.4/1, in good agreement with that predicted by *Lingenfelter* [1963] for this period in the solar activity cycle. The mean efficiency of the Ogo 6 neutron detector was assumed to be independent of latitude, although there was a 2% variation introduced from changes in the energy spectrum of leakage neutrons with latitude.

The change in neutron rate N_G' with the altitude can be expected to depend upon the latitude at which the measurements were taken. This is a result of latitude mixing, i.e., neutrons from a wider range of latitudes contribute to the counting rate as the altitude is increased. Since the altitude variation as seen by the Ogo 6 detector is much smaller than the latitude variation, the latitude variations must be correctly evaluated before determining the altitude variation. The data presented here used the predicted latitudes for the Ogo 6 spacecraft, which may be in error by several degrees. Such systematic errors can greatly affect the altitude variation of neutron rate N_G' at latitudes where the neutron flux changes rapidly with latitude.

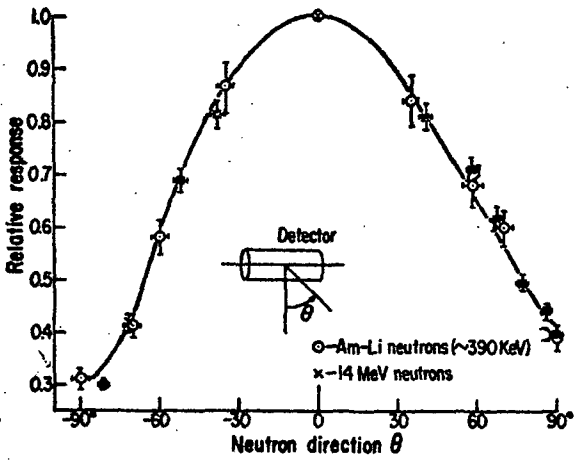

Fig. 3. Angular dependence of efficiency of detector.

For these reasons we limit our present examination of the altitude dependence of neutrons to latitudes greater than 70°, where the neutron flux can be seen to be constant over latitude (Figure 4).

The altitude dependence of N_G' for these latitudes is shown in Figure 5. The mean decrease in count rate N_G' between 450 and 950 km is 26.0 ± 4.6% (rms error). Written in terms of a radial dependence of neutron count rate, this becomes $N_G'(R) = AR^{-4.8 \pm 0.9}$, where R is the distance from the center of the earth. For comparison, an altitude variation in N_G' expected for a completely vertical neutron flux ($R^{-2.0}$ altitude dependence) is shown in Figure 5. A vertical neutron flux disagrees with our observations (probability of chi-squared greater than observed is 0.005). Our observations are not in disagreement with the altitude variation $R^{-3.0}$ between 450 and 950 km altitude expected for an isotropic neutron flux at the top of the atmosphere (probability of chi-squared greater than observed is 0.16). Taking the significance level in chi-squared to be 0.05, our observations agree with angular distributions of neutron flux that are flatter than cos θ, where θ is the angle from the vertical. For our purposes here, we have assumed an isotropic neutron flux at the top of the atmosphere.

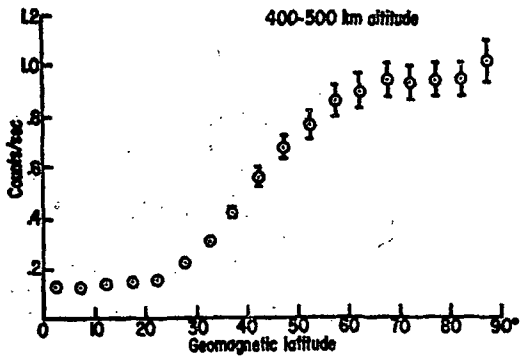

Fig. 4. Latitude dependence of neutron counting rate N_G' for altitudes between 400 and 500 km.

Neutron leakage flux at the top of the atmosphere. To determine the leakage flux at the top of the atmosphere, the observed neutron rates between 400 and 500 km, denoted $N_G'(450)$, were reduced to the top of the atmosphere (taken to be 50 km) by using the calculated altitude dependence expected for an isotropic neutron flux distribution at the top of the atmosphere. This amounted to a mean correction of 43%. Then the counting rate at 50 km, $N_G'(50)$, was converted to the leakage flux ϕ_L, by using the relationship $\phi_L = 0.5N_G'(50)/\langle\epsilon\rangle$ for a 2π-isotropic neutron flux distribution, where $\langle\epsilon\rangle$ is the mean efficiency. This same relationship was used by *Haymes* [1964] and *Holt et al.*, [1966], who had detectors responding primarily to 1- to 10-Mev neutrons. Other experiments using detectors sensitive primarily to neutrons of lower energy [*Bame et al.*, 1963; *Boella et al.*, 1965; *Lockwood and Friling*, 1968] have determined the neutron flux $\phi = N/\langle\epsilon\rangle$. This is equal to the leakage flux only for the case of an angular distribution

TABLE 2. Total Leakage Neutron Fluxes Found from the Ogo 6 Experiment and Several 1- to 10-Mev Experiments.

Latitude, degrees	Experiment	Flux Found with Lingenfelter Spectrum*	Flux Found with Newkirk Spectrum*
7.4	Ogo 6	0.06 ± 0.01	0.07 ± 0.01
8	*Holt et al.* [1966]	0.09	0.06
42.3	Ogo 6	0.25 ± 0.03	0.30 ± 0.04
41.5	*Haymes* [1964]	0.36 ± 0.03	0.24 ± 0.03
42	*Holt et al.* [1966]	0.36	0.24
68.1	Ogo 6	0.42 ± 0.05	0.52 ± 0.06
68	*Holt et al.* [1966]	0.84	0.64

* The *Lingenfelter* [1963] and *Newkirk* [1963] energy spectra for leakage neutrons.

in which all the neutrons are moving vertically upward at the top of the atmosphere. As seen in the preceding section, such an angular distribution is not compatible with the observed altitude dependence in neutron counting rate.

In Table 2 are given total neutron fluxes for the Ogo 6 detector, computed from the rates N_6' by using the mean efficiencies for the *Lingenfelter* [1963] and *Newkirk* [1963] energy spectra of leakage neutrons. Also shown are total neutron fluxes obtained from measurements in the 1- to 10-Mev region by *Haymes* [1964] and *Holt et al.*, 1966]. The 1- to 10-Mev measurements have had several corrections applied to them, to compare them with the Ogo 6 results. First, the values were corrected to the same period in the solar-activity cycle by using the Mt. Washington neutron monitor rate and the calculated relative leakage fluxes between solar maximum and minimum [*Lingenfelter*, 1963]. Second, the 1- to 10-Mev neutron fluxes were multiplied by the ratio of total to 1- to 10-Mev neutrons given by the appropriate neutron energy spectrum (Lingenfelter or Newkirk) to determine a total neutron leakage flux.

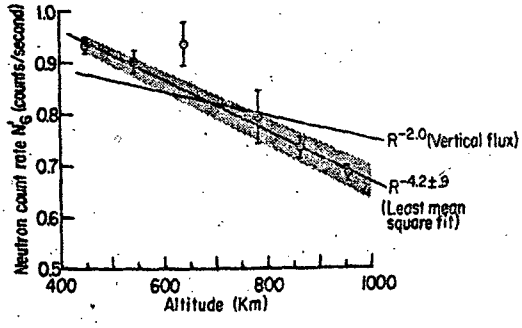

Fig. 5. Altitude dependence of neutron counting rate N_6' for latitudes > 70°.

It can be seen from Table 2 that the total neutron fluxes found from the 1- to 10-Mev measurements and the lower energy Ogo 6 measurements are in closer agreement if the Newkirk spectrum of leakage neutrons in the vicinity of spectrum is used. If the Lingenfelter spectrum is used, the 1- to 10-Mev measurements yield fluxes that are as much as twice the corresponding Ogo 6 flux, thus indicating that the energy 1 Mev is harder than that calculated by Lingenfelter.

In Figure 6 the values of total neutron leakage flux ϕ_L, found for the Ogo 6 detector by using the Newkirk energy spectrum of leakage neutrons, are plotted as a function of geomagnetic latitude.

The other experimental values (Figure 6) were corrected for solar modulation to compare them with the present results. They were also corrected for altitude by using the altitude dependence expected for an isotropic neutron flux distribution at the top of the atmosphere. Where necessary, they were adjusted to the neutron leakage flux dependence on counting rate given by $\phi_L = 0.5\ N/\langle\epsilon\rangle$. Finally, the Newkirk energy spectrum has been used with the published efficiency versus energy curves for these experiments to derive the neutron flux from the counting rates.

The total neutron leakage flux measurements reported for the Ogo 6 detector are in agreement with the other experimental observations (Figure 6). Also, the measurements reported for the 1- to 10-Mev experiments agree with the lower energy measurements when the Newkirk energy spectrum is used. This is not true for the Lingenfelter energy spectrum (Table 2). Spectral measurements in the 1- to 10-Mev region [*Haymes*, 1964; *Holt et al.*, 1966] have

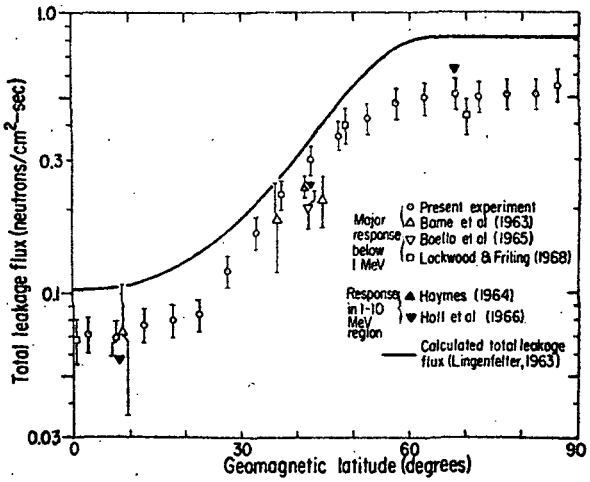

Fig. 6. Neutron albedo flux as a function of latitude.

found an energy spectrum similar to or slightly harder than the Newkirk spectrum.

The total neutron leakage flux as a function of latitude given by *Lingenfelter* [1963] plotted in Figure 6 gives the same calculated intensity as that of Newkirk at 57°, where the Newkirk calculation was made. The experimental observations of total leakage flux in Figure 6 are 0.7 times the predicted values. This result is consistent with the observations of *Miles* [1964] on the neutron densities in the atmosphere, which gave values 0.6 times that derived from the Lingenfelter calculations.

Summary

The present results regarding the neutron leakage flux indicate the following: a total neutron leakage flux of 0.7 times the intensity predicted by *Lingenfelter* [1963] and *Newkirk* [1963]; a latitude variation similar to that given by *Lingenfelter* [1963]; an energy spectrum below 10^7 ev similar to that given by *Newkirk* [1963]; an angular distribution of neutrons at the top of the atmosphere which may be isotropic over 2π but in any case is unlikely to be more peaked toward the vertical than a cos θ distribution, where θ is the angle from the vertical.

Acknowledgments. We would like to thank Messrs. G. Spellman, R. Hill, and the staff of Time-Zero, Inc., for their part in the design and construction of the detection system; Mrs. S. Dewdney and Mr. W. Dotchin of the University of New Hampshire, and Dr. R. Robinson and the staff of the Oak Ridge National Laboratories for their help in performing the calibrations; and the staff of TRW Systems, Inc., for their assistance during the spacecraft integration period.

This work is supported by the National Aeronautics and Space Administration under contract NAS5-9313.

* * *

The Editor wishes to thank R. C. Haymes and R. E. Lingenfelter for their assistance in evaluating this paper.

References

Bame, S. J., J. P. Conner, F. B. Brumley, R. L. Hostetler, and A. C. Green, Neutron flux and energy spectrum above the atmosphere, *J. Geophys. Res., 68,* 1221–1228, 1963.

Boella, G., G. Degli Antoni, C. Dilworth, M. Panetti, and L. Scarsi, Measurement of the cosmic ray neutron flux at 4.6 billion volts geomagnetic cutoff rigidity, *J. Geophys. Res., 70,* 1019–1030, 1965.

Geiger, K. W., and C. K. Hargrove, Neutron spectrum of Am^{241}-Be(α, n) source, *Nucl. Phys., 53,* 204–208, 1964.

Haymes, Robert C., Fast neutrons in the earth's atmosphere, *J. Geophys. Res., 69,* 841–852, 1964.

Hanson, A. O., Radioactive neutron sources, in *Fast Neutron Physics, 1,* edited by J. B. Marion and J. L. Fowler, Interscience, New York, 1960.

Holt, S. S., R. B. Mendell, and S. A. Korff, Fast neutron latitude variations in the atmosphere at solar minimum, *J. Geophys. Res., 71,* 5109–5116, 1966.

Lingenfelter, R. E., The cosmic ray neutron leakage flux, *J. Geophys. Res., 68,* 5633–5639, 1963.

Lockwood, J. A., E. L. Chupp, and R. W. Jenkins,

Cosmic-ray neutron monitor for Ogo-F, *IEEE Trans. Geosci. Electron., GE-7*, 88–93, 1969.
Lockwood, J. A., and L. A. Friling, Cosmic ray neutron measurements above the atmosphere, *J. Geophys. Res., 73*, 6649–6663, 1968.
Miles, Ralph F., Density of cosmic ray neutrons in the atmosphere, *J. Geophys. Res., 69*, 1277–1284, 1964.
Newkirk, L. L., Calculation of low-energy neutron flux in the atmosphere by the Sn method, *J. Geophys. Res., 68*, 1825–1833, 1963.
Solar Geophysical Data, Environmental Science Services Administration, July-August, 1969.
Tatsuta, H., K. Katoh, and Y. Yoshida, Energy response of BF_3 counter using paraffin moderators, *Japan J. Appl. Phys., 4*, 321–325, 1965.

(Received March 13, 1970.)

The Energy Dependence of the Cosmic-Ray Neutron Leakage Flux in the Range 0.01–10 Mev

R. W. JENKINS,[1] S. O. IFEDILI, J. A. LOCKWOOD, AND H. RAZDAN[2]

University of New Hampshire, Physics Department, Durham 03824

The cosmic-ray neutron leakage flux and energy spectrum in the range 1–10 Mev were measured by a neutron detector on the Ogo 6 satellite from June 7 to September 30, 1969. The same detector simultaneously measured the total leakage flux, having 75% of its response to the leakage flux in the interval 1 kev to 1 Mev. For a neutron energy spectrum of the form $AE^{-\gamma}$ in the range 1–10 Mev, the upper limit to γ for polar regions ($P_c \lesssim 0.3$ Gv) was found to be 1.0 and for the equatorial regions ($P_c \gtrsim 12$ Gv) was 1.2. For the polar regions, the lower limit to γ was found to be 0.8. This energy spectrum at 1–10 Mev is slightly flatter than L. L. Newkirk predicted. The neutron fluxes at 1–10 Mev were 0.28 ± 0.03 and 0.035 ± 0.003 cm^{-2} sec^{-1} for $P_c \lesssim 0.3$ and $P_c \gtrsim 12$ Gv, respectively. The ratios of the neutron flux at 1–10 Mev to the total neutron flux were 0.54 ± 0.07 for $P_c \gtrsim 0.3$ Gv and 0.50 ± 0.06 for $P_c > 12$ Gv.

The energy spectrum of the cosmic-ray neutron leakage flux in the range 1–10 Mev has been measured by several workers [*Haymes*, 1964; *Baird and Wilson*, 1966; *Holt et al.*, 1966; *Albernhe and Talon*, 1969; and *Merker et al.*, 1970] who used detectors sensitive to neutrons through the production of knock-on protons. These measurements have been compared with lower-energy measurements made at other times [*Jenkins et al.*, 1970] in order to extend the knowledge of the energy spectrum to the range 0.001–10 Mev. In the present paper we report the results of four months of simultaneous measurements of leakage neutrons in the ranges 1–10 Mev and 0.001–1 Mev made with the University of New Hampshire neutron detector on the polar-orbiting Ogo 6 satellite. From these data, information is deduced about the energy spectrum in the range 0.001–10 Mev and its variation with latitude.

DETECTOR

The neutron detector used has been described in detail by *Lockwood et al.* [1969] and *Jenkins et al.* [1970]. It consists of a ^{3}He-filled proportional counter, which is sensitive mainly to slow neutrons through the reaction $^3He\ (n, p)^3H$ and is surrounded by a plastic scintillator and a ring of charged-particle guard counters. The plastic scintillator serves two functions; first, to slow down faster neutrons so that they can be detected more efficiently by the ^{3}He counter; and, second, to measure the neutron energy spectrum in the range 1–10 Mev with a four-channel pulse-height analyzer. The neutron energy distribution is deduced from the pulse-height distribution of scintillation events followed within 25 μsec by a ^{3}He-counter event. The charged-particle guard counters act as an anticoincidence shield against cosmic-ray nuclei that may produce detectable neutrons in the material adjacent to the ^{3}He counter. Data obtained include the total counting rate of the ^{3}He-filled counter (TN), the rate of ^{3}He-counter events not gated off by the charged-particle guard counters (GN), and the rates of events in the four scintillation channels that precede GN events by less than 25 μsec (PHA 1, 2, 3, and 4).

The efficiencies of the ^{3}He counter (GN) and four scintillator channels (PHA 1, 2, 3, and 4) were measured at energies from 5 kev to 20 Mev with a 5.5-Mev Van der Graaf accelerator. The efficiency is plotted in Figure 1 as a function of energy for the ^{3}He-counter events. (The details of the efficiency calibrations are given by *Jenkins et al.* [1970].) Energy spectra calculated for the cosmic-ray leakage neutron flux

[1] Now at Communications Research Center, Ottawa, Ontario, Canada.

[2] On leave from High Altitude Research Laboratory, Gulmarg, India.

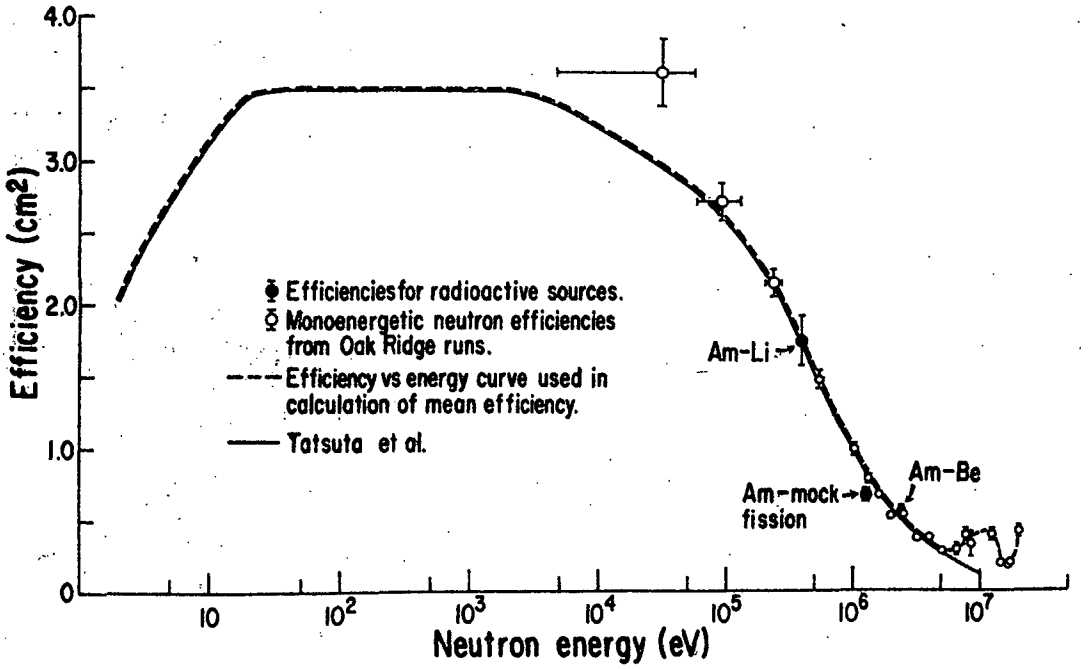

Fig. 1. ^{3}He neutron counter efficiency as a function of energy. The details on these measurements are presented by *Jenkins et al.* [1970].

[*Newkirk*, 1963; *Lingenfelter*, 1963] were used to deduce mean efficiencies for the ^{3}He counter [*Jenkins et al.*, 1970]. From these efficiencies the observed counting rates (GN) can be converted to a total neutron leakage flux. For either the Newkirk or Lingenfelter spectra, the ^{3}He counter was found to respond mainly to neutrons between 10 kev and 1 Mev.

The efficiency as a function of energy for the scintillator channels PHA 1, 2, 3, and 4 is shown in Figure 2. Although the upper discrimination levels were set below 10-Mev energy loss, there is a finite efficiency for neutrons of energies above 10 Mev because of the contribution of inelastic carbon collisions to the slowing down of higher-energy neutrons in the scintillator. Uncertainties in the measured efficiencies of PHA 1, 2, 3, and 4 are 18%, 16%, 8%, and 11%, respectively.

DATA REDUCTION

The data were obtained between June 7 and September 30, 1969, and have been sorted according to spacecraft position. In this paper we are concerned principally with two regions:

1. Polar region, where the cosmic-ray vertical cutoff rigidity P_c at the earth's surface is <0.3 Gv and altitude is between 400 and 500 km.
2. Equatorial region, where P_c is $\gtrsim 12$ Gv and altitude is between 400 and 600 km.

The counting rates GN and PHA 1, 2, 3, and 4 were corrected for a small background arising from neutrons produced locally in the spacecraft and surrounding detector material by cosmic rays, and also arising from highly ionizing cosmic rays whose energy loss in the ^{3}He counter is above threshold. The present background correction represents a revision of the correction applied in a previous paper [*Jenkins et al.*, 1970]. However, both the present correction (5% for GN) and previous correction (12% for GN) are small enough that the conclusions of that paper are not changed. The details of the background correction are given in Appendix 1.

After corrections for background, the rates GN and PHA 1, 2, 3, and 4 were reduced to the top of the atmosphere (taken to be at 50-km altitude), using the altitude dependence calcu-

lated for our detector assuming a 2π isotropic angular distribution of leakage neutrons at the top of the atmosphere. From the counting rates at the top of the atmosphere and the measured efficiencies, we then calculated the fluxes of leakage neutrons, again assuming an isotropic angular distribution for the neutrons leaking out of the atmosphere.

Spectral Shape in the Range 1–10 Mev

The scintillator rates PHA 1, 2, 3, and 4 were used to examine the shape of the neutron leakage spectrum at 1–10 Mev. An energy spectrum of the form $AE^{-\gamma}$ was assumed and was folded together with the scintillator efficiency curves of Figure 2 to derive the expected counting rates of PHA 1, 2, 3, and 4 for various values of A and γ. The expected and observed rates were then compared in both the polar and equatorial regions by a χ^2 test to determine which values of A and γ best fitted the observations. The results of this test for the polar region data in June 1969 are shown in Figure 3. Contour lines representing boundaries to the regions within which 60% and 90% of the allowed values of A and γ must fall are shown. From this graph it is clear that any spectral shape flatter than E^{-1} fits our data. This is a consequence of the finite efficiencies of four scintillator channels at neutron energies above 10 Mev and the observed counting rates. The neutron leakage flux in the energy region 1–10 Mev, computed from the allowed values of A and γ for the polar region in June 1969, is 0.28 ± 0.03 neutrons cm^{-2} sec^{-1} (Table 1). An upper limit (at the 95% confidence level) to the steepness of the energy spectrum $\gamma_{max} = 1.07$ is found. The rest of the results for the four months of polar and equatorial regions are presented in Table 1. The neutron fluxes at 1–10 Mev in both regions for the four months agree within the given rms errors. Generally, a

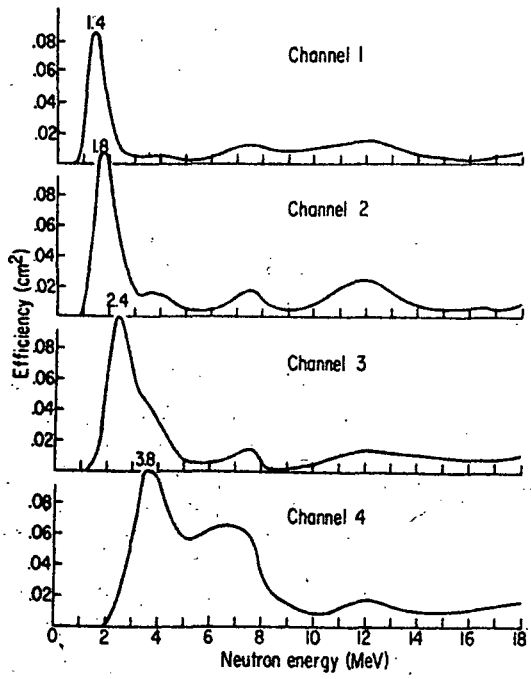

Fig. 2. Neutron efficiencies as a function of energy for the four scintillator channels (PHA 1, 2, 3, and 4).

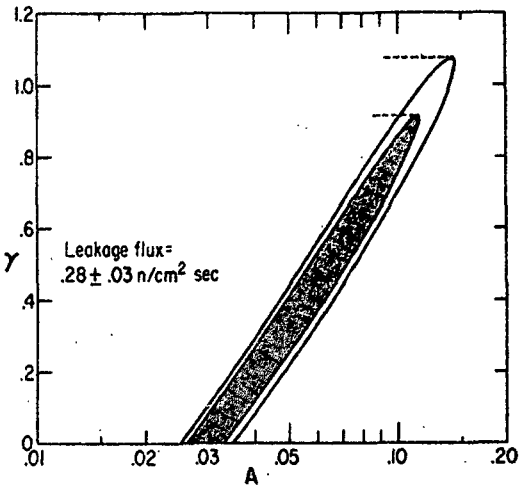

Fig. 3. Fit of $AE^{-\gamma}$ to the neutron PHA results for June 1969 at $P_c \lesssim 0.3$ Gv and altitudes <500 km. All data reduced to 50 km, using an altitude correction to the neutron counting rates. Contour line for boundaries to regions within which 60% and 90% of allowed values must fall are shown.

TABLE 1. The Upper Limit to $\gamma(\gamma_{max})$ and 1–10 Mev Neutron Leakage Flux ($N_{1-10} = \int_1^{10} AE^{-\gamma}\, dE$)

Month (1969)	Polar Region		Equatorial Region	
	γ_{max}	N_{1-10}, cm^{-2} sec^{-1}	γ_{max}	N_{1-10}, cm^{-2} sec^{-1}
June	1.07	0.28 ± 0.03	1.28	0.032 ± 0.003
July	0.95	0.26	1.12	0.035
Aug.	0.88	0.28	1.07	0.036
Sept.	1.02	0.27	0.85	0.032

TABLE 2. Comparison of Normalized Predicted Counting Rates and Observed Rates (sec^{-1}) for the Four Scintillator Channels PHA 1, 2, 3, and 4 in June 1969

Channel	Predictions				Observations
	Newkirk, 1963	*Lingenfelter*, 1963	*Wilson et al.*, 1969	*Merker*, 1970	
	Equatorial Region ($P_c > 12$ Gv)				
PHA 1	0.0020±0.0004	0.0026±0.0005	0.0019±0.0003	0.0021±0.0004	0.0020±0.0002
PHA 2	0.0026±0.0004	0.0030±0.0005	0.0025±0.0004	0.0027±0.0004	0.0022±0.0003
PHA 3	0.0022±0.0002	0.0021±0.0002	0.0023±0.0002	0.0022±0.0002	0.0019±0.0002
PHA 4	0.0029±0.0003	0.0020±0.0002	0.0030±0.0003	0.0027±0.0003	0.0034±0.0003
χ^2 (3 deg freedom)	3.2	16.8	2.5	5.1	
Significance of fit, %	40	<0.1	45	15	
	Polar Region ($P_c < 0.3$ Gv)				
PHA 1	0.017±0.003	0.024±0.004	0.016±0.003	0.019±0.003	0.015±0.001
PHA 2	0.023±0.004	0.028±0.004	0.022±0.003	0.024±0.004	0.019±0.001
PHA 3	0.020±0.002	0.020±0.002	0.020±0.002	0.020±0.002	0.018±0.001
PHA 4	0.026±0.003	0.019±0.002	0.027±0.003	0.024±0.003	0.030±0.001
χ^2 (3 deg freedom)	4.8	34.6	3.2	9.0	
Significance of fit, %	20	<0.1	35	3	

lower γ_{max} is found in the polar than in the equatorial region, but this is not significant in light of the larger statistical errors in the equatorial region.

A second technique was used to test the published calculations of leakage neutron energy spectra. The spectral distributions calculated by *Newkirk* [1963], *Lingenfelter* [1963], *Wilson et al.* [1969], and *Merker* [1970] were folded together with the scintillator efficiencies and normalized so that the best fit to our observations would be obtained. The normalized predictions and the observed rates (PHA 1, 2, 3, and 4) were then compared. The results for June 1969 are shown in Table 2. The Lingenfelter spectral shape, given by $E^{-1.6}$ in the energy range 1–10 Mev, does not fit our observations. The Newkirk spectrum, which can be approximated by $E^{-1.0}$ in this energy interval, is a fair fit to the June data. The more recent calculations of *Wilson et al.* [1969], in which some structure in the spectrum is evident, fit the June data possibly better than the Newkirk calculations. The Wilson calculation, however,

TABLE 3. Fit of *Newkirk* [1963] and *Wilson et al.* [1969] Spectra to the Observed PHA Counting Rates for June–September 1969

Month (1969)	Equatorial Region				Polar Region			
	Newkirk		Significance level* Wilson et al.		Newkirk		Significance level* Wilson et al.	
	χ^2	%	χ^2	%	χ^2	%	χ^2	%
June	3.2	40	2.5	45	4.8	20	3.2	35
July	3.6	30	2.2	55	7.9	5	5.7	15
Aug.	6.0	10	5.0	20	10.1	1	7.6	5
Sept.	10.1	1	7.6	5	6.4	10	4.5	20

* 3 degrees of freedom.

TABLE 4. Comparison of the Fast Neutron Leakage Flux (N_{1-10}) with the Total Leakage (N_T) using *Newkirk's* [1963] Energy Spectrum

Month (1969)	Polar Region			Equatorial Region			$(N_P/N_T)_{poles} - (N_P/N_T)_{eq}$
	N_P	N_T	N_P/N_T	N_P	N_T	N_P/N_T	
June	0.30 ± 0.02	0.56 ± 0.06	0.54 ± 0.07	0.034 ± 0.003	0.076 ± 0.0008	0.45 ± 0.06	+0.090 ± 0.025
July	0.29	0.55	0.54	0.039	0.077	0.51	+0.028
Aug.	0.32	0.56	0.57	0.040	0.077	0.53	+0.040
Sept.	0.30	0.58	0.51	0.039	0.079	0.50	+0.012
Predicted ratio at λ ~ 57°N			0.45				

extends only to 10 Mev. Contributions to the counting rate from above this energy were ignored for this spectrum. Both these spectra are slightly steeper than the observations would indicate. The Merker spectrum is a poor fit, being too steep for the observations.

The fit of the observed PHA counting rates to the Newkirk and Wilson et al. spectra is generally poorer for the later months (Table 3). The observed counting rates in the PHA channels for all four months agree within the statistical fluctuations. Therefore we must conclude that the Newkirk and Wilson et al. spectra are only poor fits to the observed data. From the relative counting rates in the four channels, a flatter energy spectrum than those calculated is indicated for the later months as well.

Comparison of Neutron Flux at 1–10 Mev with Total Neutron Flux

Information about the energy spectrum of the leakage neutrons can be extended to lower energies by comparing the scintillator measurements (PHA 1, 2, 3, and 4) with the ^{3}He-counter measurements (GN). From the normalization constants used in fitting the calculated spectra of *Newkirk* [1963] and *Lingenfelter* [1963] to the observed scintillator counting rates, leakage fluxes in the region 1–10 Mev (fast neutrons) were obtained for each of these spectra. The total leakage fluxes were obtained by converting the ^{3}He-counter rate to a flux using the corresponding neutron efficiencies deduced for each of the two spectra. The ratio of fast neutron leakage flux to total leakage flux thus found from the scintillator and ^{3}He-counter rates was then compared with the ratios predicted directly from the *Lingenfelter* [1963] and *Newkirk* [1963] spectra.

For the Lingenfelter spectrum, the predicted ratio of fast neutron leakage flux to total neutron leakage flux near the poles is 0.32, in contrast to the measured ratio for the June data of 0.68 ± 0.09. Similarly, for the equatorial region the calculated ratio is 0.32 and the measured ratio (June) is 0.54 ± 0.07. Thus the Lingenfelter spectrum does not predict a sufficiently high fraction of leakage neutrons at 1–10 Mev for the present measurements. This result supports the preliminary results [*Jenkins et al.*, 1970] in which the ^{3}He-counter measurements were compared with the fast neutron measurements made by other workers [*Haymes*, 1964; *Holt et al.*, 1966].

Better agreement between the predicted and measured ratio of fast neutron leakage flux to

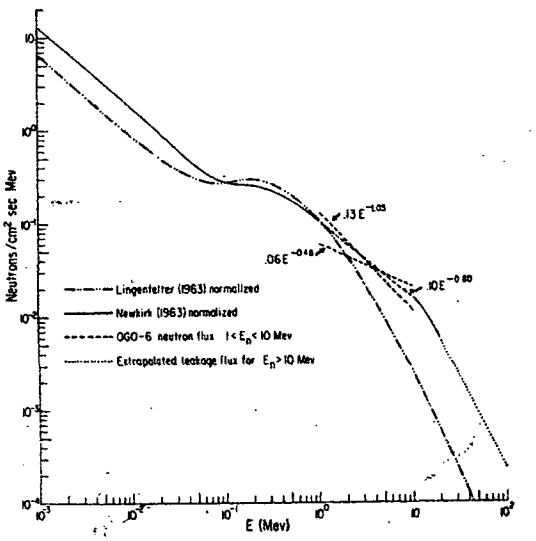

Fig. 4. Differential neutron energy spectra. The Lingenfelter and Newkirk spectra have been normalized to the Ogo 6 measured neutron flux for $E < 1$ Mev. Above E = 10 Mev the spectrum is assumed to be of the form $E^{-\alpha}$.

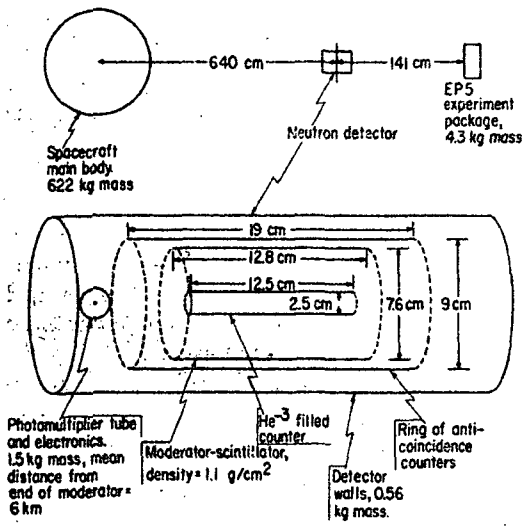

Fig. 5. Geometry of the neutron detector used to calculate the neutron production in the detector.

total neutron leakage flux is obtained using the *Newkirk* [1963] spectrum (Table 4). For the equatorial regions the Newkirk spectral shape agrees with our measurements. For the polar region the result suggests that there are relatively more fast neutrons than the Newkirk spectral shape (originally calculated for a geomagnetic latitude of 57°N) predicts. The increase in the observed ratio of fast-to-total leakage flux from the equator to the poles is also listed in Table 4. A relatively small error arises because the large errors in detector efficiency contribute in the same way to errors in the ratio at both positions; i.e., the efficiency error expressed as a fraction is constant. This enrichment of the fast neutron leakage spectrum is seen in the calculations of *Lingenfelter* [1963]; however, the observed change is greater. *Boella et al.* [1965] interpreted his observed variation of latitude effect with atmospheric depth as being due to more of the neutron sources being close to the top of the atmosphere at high latitudes, and anticipated a resultant enrichment of the 1- to 10-Mev leakage flux at high latitudes.

Finally, the measurements of the total neutron leakage flux and the neutron leakage flux at 1–10 Mev can be used in conjunction with information on the spectral shape for $E < 1$ Mev and $E > 10$ Mev to check the measured values of γ in the interval 1–10 Mev. For the polar regions, the minimum value of χ^2 yields a 1- to 10-Mev leakage flux given by $N(E) = 0.06E^{-0.43}$ neutrons cm^{-2} sec^{-1}. Let us consider how this spectrum fits the calculated spectra at lower energies. For the Newkirk neutron energy spectrum, 87% of the counting rate of the Ogo 6 ^{3}He detector is contributed by neutrons with $E < 1$ Mev [*Jenkins et al.*, 1970]. Therefore let us normalize the Newkirk spectrum of $E < 1$ Mev by the ratio of the neutron flux measured by the Ogo 6 to the total flux at 0 g/cm^2 calculated by Newkirk. The Newkirk spectrum for $E < 1$ Mev normalized by this ratio (0.560/0.899) is shown in Figure 4. For the Lingenfelter spectrum, 81% of the counting rate of the Ogo 6 detector arises from neutrons $E < 1$ Mev. Thus we can normalize the Lingenfelter neutron leakage spectrum for sunspot minimum and $\lambda > 80°$ by the ratio of the measured total leakage flux to the calculated flux (0.460/1.367) as shown in Figure 4. It is known that for $E < 10$ kev the spectrum goes as E^{-1}, and the only differences in the two spectra are for $E > 10$ kev. However, at $E = 1$ Mev, $N(E)$ for the normalized spectra are equal. Consequently, the differential spectrum for $1 < E < 10$ Mev is most probably given by $0.10\ E^{-0.80}$, or as steep as $0.13\ E^{-1.05}$. Any spectrum as flat as $E^{-0.43}$ does not merge with either the Lingenfelter or Newkirk spectra for $E < 1$ Mev. For a flat spectrum the leakage flux for $E \geq 10$ Mev is much larger than that calculated by Lingenfelter. For either the normalized Lingenfelter or Newkirk spectra in Figure 4, the ratio of the leakage flux at 1–10 Mev to the total leakage flux is 0.46, in approximate agreement with the observed value. Therefore, for the polar regions the lower limit

TABLE 5. Corrections to the ^{3}He-Counter Gated Counting Rate (counts per second) at 750-km Altitude for $P_c \pm 0.3$ Gv

Locally produced neutrons	
In the spacecraft	0.002
In the neighboring electronics and detector walls	0.014
In the moderator	0.002
Highly ionizing events in the ^{3}He counter	
Low-energy cosmic-ray protons	0.005
Low-energy cosmic-ray α particles	0.010
$Z \leq 3$ cosmic rays (including showers)	0.008
Evaporation protons from cosmic-ray interactions	0.001
Proton and α-initiated shower particles	0.000
Total correction (estimated uncertainty, +30%)	0.042

to γ is 0.8, with the most probable value $0.8 < \gamma < 1.0$ for the interval 1–10 Mev.

SUMMARY

We are able to set the limits on γ in the polar neutron energy spectrum ($AE^{-\gamma}$, $1 < E < 10$ Mev) as $\gamma_{max} = 1.0$ and $\gamma_{min} = 0.80$. This agrees with the results of *Holt et al.* [1966] and *Merker et al.* [1970], who found $\gamma = 1.05 \pm 0.15$ and $\gamma = 1.08 \pm 0.10$, respectively, near the top of the atmosphere in the same energy range. Our measured upper limit for γ indicates a flatter spectrum than the value $\gamma = 1.3 \pm 0.10$ at 41.5°N measured by *Haymes* [1964]. The measurements by *Baird and Wilson* [1966] of the 1- to 10-Mev spectrum on a rocket yield $\gamma = 0.8 \pm 0.3$, essentially in agreement with our results. A slightly steeper spectrum ($\gamma = 1.24$) was deduced by *Albernhe and Talon* [1969] for the range 3–14 Mev. However, no errors on γ were given. There is fair agreement with the leakage spectrum calculated by *Newkirk* [1963] and *Wilson et al.* [1969] in the fast-neutron range (1–10 Mev).

The measured ratio of fast neutron leakage to the total leakage increases slightly between the equator and poles. The observed ratio near the equator agrees with calculations by *Newkirk* [1963] done for a latitude of 57°N, but near the poles the ratio indicates that there is a greater fraction of fast neutrons that the Newkirk calculation predicts.

APPENDIX: CORRECTIONS

Background correction of the ^{3}He-counter rate. The corrections to the ^{3}He gated counting rate that are needed before it can be used to determine the leakage neutron fluxes arise from the following types of events.

a. Neutrons produced locally in the spacecraft, adjacent electronic circuitry, and moderator by cosmic rays escaping detection in the anticoincidence guard counts.

b. Charged particles entering the unguarded ends of the ^{3}He counter, which, by their high ionization loss in the ^{3}He counter, produce voltage pulses above discriminator threshold. The following particle events fall into this classification:

1. Cosmic-ray protons with original energy between 100 and 125 Mev.
2. Cosmic-ray α particles with original energy between 100 and 375 Mev/nucleon.

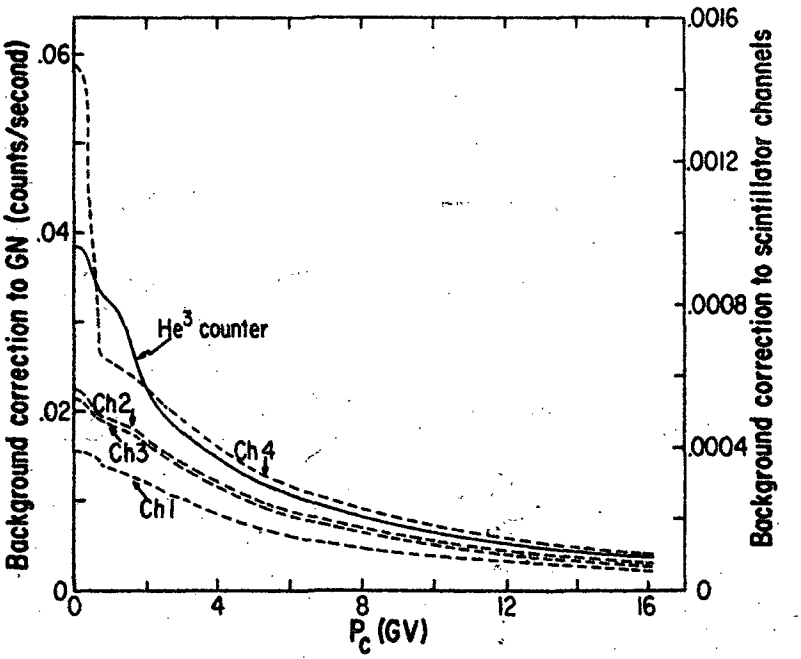

Fig. 6. Background corrections to the counting rates of the ^{3}He counter (GN) and the scintillator channels (PHA 1, 2, 3, and 4) as a function of vertical cutoff rigidity (P_c).

TABLE 6. Background Contributions (per cent) to the Counting Rate of the Scintillator PHA Channels for the Polar Region

Particles	PHA 1	PHA 2	PHA 3	PHA 4
Locally produced neutrons	3.6	3.8	3.7	3.0
Low-energy protons	0.2	0.5	0.6	3.5
Total	3.8	4.3	4.3	6.5

3. Cosmic-ray L, M, and H nuclei of all energies sufficient to reach the ^{3}He counter.
4. Evaporation protons produced in the moderator and walls of the ^{3}He counter by cosmic rays.
5. Shower particles produced in nuclear interactions of the cosmic rays with the moderator and walls of the ^{3}He counter.

Corrections to the ^{3}He-counter gated counting rate were evaluated for these sources with the cosmic-ray fluxes given by *Webber* [1967] corrected to the present time in the solar activity cycle by using the Mount Washington neutron monitor intensity. The cosmic-ray cutoff rigidities (P_c) were evaluated from the tables given by *Shea et al.* [1968]. The neutron production cross sections and resulting energy distributions of the locally produced neutrons were taken from *Chen et al.* [1955], *Dostrovski et al.* [1958], *Jain et al.* [1959], *Jain* [1961], *Bercovitch et al.* [1960], *Bertini* [1965], and *Alsmiller et al.* [1967]. The geometry used for these calculations is shown in Figure 5.

Partial corrections calculated for the polar region at 750 km altitude are listed in Table 5. The total correction as a function of geomagnetic cutoff is plotted in Figure 6.

Background correction of the scintillator rates. A scintillator output pulse will occur for several of the types of ^{3}He-counter background events listed above. However, since the uppermost discrimination level on the scintillator corresponds to a 10-Mev proton energy loss, the geometry involved excludes a large fraction of the background because the events correspond to more than a 10-Mev proton energy loss in the scintillator. Only a small fraction of the cosmic-ray protons counted by the ^{3}He detector as GN events have a sufficiently small scintillator light output to be counted as PHA events. The contribution from particles with $Z > 2$ is negligible. On the other hand, the locally produced neutrons having energies between 1 and 15 Mev can contribute to the PHA events.

The contribution to the counting rates PHA 1, 2, 3, and 4 of the scintillator from locally produced neutrons was determined by assuming an evaporation energy spectrum. The spectrum of *Alsmiller et al.* [1967] for evaporation neutrons produced by 400-Mev protons incident on aluminum was assumed. Then the relative contributions (f_{GN}, f_i, $i = 1, 2, 3, 4$) of these neutrons to the counting rates GN and PHA 1, 2, 3, and 4 were evaluated from the measured efficiency curves. The absolute contribution of locally produced neutrons to the PHA 1, 2, 3, and 4 rates was then determined by putting $R_i = (f_i/f_{GN})\ R_{GN}$, where R_{GN} is the absolute contribution of background to the gated neutron rate.

The low-energy proton contributions to the PHA counting rates were deduced by noting the relative increases in GN and PHA 1, 2, 3, and 4 rates that occurred in the South Atlantic anomaly, where large fluxes of protons are known to be present. From these relative increases and the normal contribution of low-energy protons to GN calculated in the preceding section, the normal contribution of low-energy protons to PHA 1, 2, 3, and 4 rates were evaluated. Table 6 lists the background corrections to the scintillator as percentages of the normal counting rate for the polar region. The corrections are less than 7% at all latitudes.

Acknowledgments. We gratefully acknowledge the assistance of Dr. E. L. Chupp in many phases of this research program. We thank Mrs. S. Dewdney, Mr. A. Buck, and Mr. R. Hart for their assistance in computer programming and in performing the calculations. The staff of the Oak Ridge National Laboratories was most helpful in performing the necessary calibrations on the Van der Graaf accelerator.

This work is supported by the National Aeronautics and Space Administration under contract NAS5-9313.

* * *

The Editor thanks R. C. Haymes and R. E. Lingenfelter for their assistance in evaluating this paper.

REFERENCES

Albernhe, F., and R. Talon, Determination of the spectrum and flux of atmospheric fast neutrons in low solar activity at a geomagnetic latitude 46°N, *Ann. Geophys., 25,* 99–102, 1969.

Alsmiller, R. G., Jr., M. Leimdorfic, and J. Bavish, Analytic representation of non-elastic cross-sections and particle emission spectra from nucleon-nucleus collisions in the energy range 25 to 400 Mev, *ORNL-4046,* Oak Ridge National Laboratory, 1967.

Baird, G. A., and B. G. Wilson, Solar minimum measurements of fast neutrons at high altitude, *Can. J. Phys., 44,* 2131–2136, 1966.

Bercovitch, M., H. Carmichael, G. C. Hanna, and E. P. Hincks, Yield of neutrons per interaction in U, Pb, W, and S_n by protons of six energies between 250 and 900 Mev selected from cosmic radiation, *Phys. Rev., 119,* 412–431, 1960.

Bertini, H. W., Results from low energy intra-nuclear-cascade calculations, *ORNL-TN-1225,* Oak Ridge National Laboratory, 1965.

Boella, G., G. Degli Antoni, C. Dilworth, L. Scarsi, G. Pizzi, and M. Tagliabue, Latitude effect on neutron albedo flux, *Nuovo Cimento, 37,* 1232–1235, 1965.

Chen, F. F., C. P. Leavitt, and A. M. Shapiro, Attenuation cross sections for 860 Mev protons, *Phys. Rev., 99,* 857–871, 1955.

Dostrovski, I., P. Rabinowitz, and R. Bivans, Monte Carlo calculations of high-energy nuclear evaporation, 1, Systematics of nuclear evaporation, *Phys. Rev., 111,* 1659–1676, 1958.

Haymes, Robert C., Fast neutrons in the earth's atmosphere, *J. Geophys. Res., 69,* 841–852, 1964.

Hess, W. N., E. H. Canfield, and R. E. Lingenfelter, Cosmic ray neutron demography, *J. Geophys. Res., 66,* 665–667, 1961.

Hess, W. N., and J. Killeen, Spatial distribution of protons from neutron decay trapped by the geomagnetic field, *J. Geophys. Res., 71,* 2799–2810, 1966.

Hess, W. N., and A. J. Starnes, Measurements of the neutron flux in space, *Phys. Rev. Lett., 5,* 48–50, 1960.

Holt, S. S., R. B. Mendell, and S. A. Korff, Fast neutron latitude variations in the atmosphere at solar minimum, *J. Geophys. Res., 71,* 5109–5116, 1966.

Jain, P. L., Angular distribution of shower particles from 1000 Bev nucleon alpha particles on emulsion nuclei, *Phys. Rev., 122,* 1890–1896, 1961.

Jain, P. L., E. Lohrmann, and M. W. Teacher, Heavy nuclei and α particles between 7 and 100 Bev/nucleon, 2, Fragmentation and meson production, *Phys. Rev., 115,* 643–654, 1959.

Jenkins, R. W., J. A. Lockwood, S. O. Ifedili, and E. L. Chupp, Latitude and altitude dependence of the cosmic-ray albedo neutron flux, *J. Geophys. Res., 75,* 4197–4204, 1970.

Lingenfelter, R. E., The cosmic-ray neutron leakage flux, *J. Geophys. Res., 68,* 5633–5639, 1963.

Lockwood, J. A., E. L. Chupp, and R. W. Jenkins, Cosmic ray neutron monitor for Ogo-F, *IEEE Trans. Geosci. Electron., GE-7,* 88–93, 1969.

Merker, M., Solar cyle modulation of fast neutrons in the atmosphere, Ph.D. Thesis, New York University, New York, 1970.

Merker, M., E. S. Light, R. B. Mendell, and S. A. Korff, The flux of fast neutrons in the atmosphere, 1, The effect of solar modulation of galactic cosmic rays, *Acta Phys. Acad. Sci. Hung., 29, Suppl., 2,* 739–744, 1970.

Newkirk, L. L., Calculation of low-energy neutron flux in the atmosphere by the S_n method, *J. Geophys. Res., 68,* 1825–1833, 1963.

Shea, M. A., D. F. Smart, and K. G. McCracken, A study of vertical cutoff rigidities using sixth degree simulations of the geomagnetic field, *J. Geophys. Res., 70,* 4117–4130, 1965.

Shea, M. A., D. F. Smart, and J. R. McCall, A five degree by fifteen degree world grid of trajectory determined vertical cutoff rigidities, *Can. J. Phys., 46,* S1098–1101, 1968.

Webber, W. R., The spectrum and charge composition of the primary radiation, *Handb. Phys., 46-2,* 181–260, 1967.

Wilson, J. N., J. J. Lambiotti, and T. Foelsche, Structure in the fast spectra of atmospheric neutrons, *J. Geophys. Res., 74,* 6494–6496, 1969.

(Received February 11, 1971;
accepted July 12, 1971.)

UPPER LIMIT TO THE 1-20 MEV SOLAR NEUTRON FLUX

J. A. Lockwood, S. O. Ifedili, and R. W. Jenkins[1]

University of New Hampshire
Physics Department
Durham, N.H. 03824

ABSTRACT

The upper limit on the quiet time solar neutron flux from 1-20 Mev has been measured to be less than 2×10^{-3} n/cm^2 sec at the 95% confidence level. This result is deduced from the OGO-6 neutron detector measurements of the "day-night" effect near the equator at low altitudes for the period from June 7, 1969, to December 23, 1969. The OGO-6 detector had very low(<4%) counting rate contributions from locally produced neutrons in the detecting system and the spacecraft and from charged-particle interactions in the neutron sensor.

[1]Now at Communications Research Center, Ottawa, Ontario, Canada.

1. INTRODUCTION

Biermann, Haxel, and Schluter (1951) first suggested that solar flare protons with energies of about 100 MeV could interact with solar atmosphere to produce a secondary flux of neutrons. Later theoretical calculations by Hess (1962), Lingenfelter et al. (1965a, b), and Lingenfelter and Ramaty (1967) gave further support to the possible existence of a solar neutron flux and showed that the only significant source of solar neutrons is from protons accelerated and slowed down during flares. For almost two decades efforts have been made to detect such a neutron flux. The measurement of a solar neutron flux is important because this is a means to evaluate some parameters of the accelerating mechanism of solar cosmic-rays such as the time scale for acceleration, the nuclear reactions which may occur, and the region in the solar envelope in which acceleration takes place. Attempts to measure this flux have been made both during small solar flares and during relatively quiet periods. The existence of a detectable solar neutron flux has not been confirmed in the searches by Hess and Kaifer (1967), Bame and Ashbridge (1966), Webber and Ormes (1967), Forrest and Chupp (1969), Zych and Frye (1969), Kim (1970), Heidbreder et al. (1970), Cortellessa et al. (1970, 1971), Daniel (1971), and Eyles et al. (1971). No attempt will be made

here to discuss all these results. For the details, reference should be made to the review of solar flare neutron production by Chupp (1971) and the survey of the experimental efforts to detect solar neutrons compiled by Lockwood (1972).

We report here the results of the OGO-6 neutron experiment which set a new lower limit to the 1-20 MeV neutrons produced at the sun during a relatively quiet period. These new measurements will be compared with others in the energy region 1-100 MeV.

2. INSTRUMENTATION

The neutron sensor used for these measurements is a moderated He^3 proportional counter surrounded by an anti-coincidence charged particle shield composed of 22 proportional counters and has a solar neutron energy response from about 10^{-1} MeV to 20 MeV. The moderator is a plastic scintillator which acts both as a moderator for fast neutrons and a detector of proton and carbon recoils produced in the slowing down of the neutrons. The neutron detecting system and its location on the OGO-6 spacecraft are shown in Figure 1. The details of the operation of the detector have been described elsewhere (Lockwood et al., 1969). Fig. 1

The neutron detector was calibrated as a function of neutron energy by exposing it to known neutron fluxes

from both Am^{241}-Li, Am^{241}-Be, and Am^{241}-mock fission radioactive sources and monoenergetic neutrons ranging from 5 keV to 20 MeV produced in reactions using the Van der Graaf accelerator at Oak Ridge National Laboratories. The neutron detector efficiency for events in the He^3 counter as a function of energy for an isotropic neutron flux is shown in Figure 2. The details of the detector calibration have been presented (Jenkins et al., 1970). The variation of the detector efficiency with the incident angle of the neutron flux was determined at neutron energies of 0.3 MeV and 14 MeV. This measured angular response curve was used to convert the measurements taken with monoenergetic neutrons incident perpendicular to the axis of symmetry of the detector into absolute efficiencies for isotropically incident neutron fluxes plotted in Figure 2. Since the response of the detector depends upon the direction of the incident neutrons, the neutron flux in space derived from the observed counting rate will depend upon the assumed angular distribution of neutrons in the vicinity of the detector.

FIG.2

3. RESULTS

The neutron counting rates were derived from those events in the He^3 proportional counter not associated with events in the charged-particle guard counters. This is referred to as the "gated" neutron counting rate. No

correction was made for background events in the He^3 counter because differences in counting rates rather than absolute counting rates were used. In any case this background rate was only about 3% at the equator (Jenkins et al., 1970, 1971). Any contributions from locally produced neutrons in the OGO-6 spacecraft were calculated to be less than 0.3%.

The data for June 7, 1969, to December 23, 1969, inclusive were first sorted according to spacecraft location. The minimum values of the charged particle counting rates for all vertical cutoff rigidities (P_c) and altitudes showed only a cutoff rigidity dependence. The ratio of the polar (P_c <0.5 Gv) to equatorial (P_c >14 Gv) minimum charged-particle rates was 4.3 to 1. To minimize the contributions from local charged-particle production the neutron rates corresponding to charged particle rates in excess of 1.5 times the minimum values for that rigidity were excluded in the analyses. The gated neutron counting rates were then sorted according to vertical cutoff rigidity and altitude into 18 vertical cutoff rigidity intervals for seven different altitude ranges. The calculated cutoff rigidity values of Shea et al. (1968) were used in this sorting. Data from the regions near the Capetown and Brazilian anomalies in the geomagnetic field were excluded from the analysis. We also eliminated data for those days on which polar particle

events were reported by detectors on Explorer 41, Pioneer 8 and Pioneer 9. The analysis for solar neutrons was restricted to only the equatorial regions for which the vertical cutoff rigidity at the earth's surface is $\geq$14 Gv. This restriction minimized the problems due to intensity - time variations and neutrons produced in the atmosphere at high latitudes by solar protons during any solar flare events which might not have been excluded. Finally, the neutron data were selected from altitudes less than 900 Km to remove neutron production effects by the energetic protons trapped in the inner radiation belt.

The differences between the neutron counting rates for the detector on the sun-ward side ("day") and for the detector completely eclipsed by the earth ("night") are listed in Table I for low altitudes and high cut-off rigidities. The errors listed are statistical and are equal to the square root of the counting rate divided by the time of measurements. There are no statistically significant differences between the two counting rates. From these data the weighted average solar neutron rate $\bar{n}_s$ in the 1-20 MeV energy range is

TABLE I

$$\bar{n}_s = \frac{\sum_{i=i}^{N} \frac{n_i}{\sigma_i^2}}{\sum \frac{1}{\sigma_i^2}} \pm \sqrt{\sum_{i=i}^{N} \sigma_i^2} \qquad (1)$$

TABLE I. DIFFERENCES IN "DAY" AND "NIGHT" NEUTRON COUNTING RATES

RIGIDITY INTERVAL (GV)	AVERAGE GEO-MAG. LAT. (°)	ALTITUDE (KM)	COUNTING RATES (/SEC) DAY	NIGHT	DIFFERENCE
14 - 16	7.5	400 - 500	0.14344 ± 0.00094	0.14670 ± 0.00220	-0.0033 ± 0.0024
> 16	0	400 - 500	0.1200 ± 0.0013	0.1178 ± 0.0021	+0.0022 ± 0.0024
14 - 16	7.5	500 - 600	0.1372 ± 0.0013	0.1417 ± 0.0029	-0.0045 ± 0.0032
> 16	0	500 - 600	0.1129 ± 0.0016	0.1177 ± 0.0031	-0.0047 ± 0.0035
14 - 16	7.5	600 - 700	0.1338 ± 0.0014	0.1340 ± 0.0025	-0.0002 ± 0.0029
> 16	0	600 - 700	0.1102 ± 0.0017	0.1104 ± 0.0030	-0.0001^{5} ± 0.0035
14 - 16	7.5	700 - 800	0.1247 ± 0.0016	0.1219 ± 0.0021	+0.0028 ± 0.0026
> 16	0	700 - 800	0.1059 ± 0.0019	0.1054 ± 0.0024	+0.0006 ± 0.0031
14 - 16	7.5	800 - 900	0.1197 ± 0.0018	0.1176 ± 0.0019	+0.0021 ± 0.0026
> 16	0	800 - 900	0.1012 ± 0.0022	0.1003 ± 0.0022	+0.0009 ± 0.0030

$$= (-1.54 \pm 9.30) \times 10^{-4}/\text{sec.}$$

Therefore, the upper limit to the continuous solar neutron rate is 1.86×10^{-3}/sec at the 95% confidence level.

The resulting upper limit continuous solar neutron flux F can be calculated from

$$F \leq \frac{1.86 \times 10^{-3}}{C\,\bar{\varepsilon}} \text{ / cm}^2 \text{ sec.} \qquad (2)$$

C is a factor which depends upon the assumed angular distribution for the neutrons incident on the detector. The mean efficiency $\bar{\varepsilon}$ in cm^2 was obtained by folding the efficiency $\varepsilon(E_n)$ for neutrons incident perpendicular to the axis of symmetry of the detector into a solar neutron energy spectrum of the shape calculated by Lingenfelter and Ramaty (1967). The shape of the solar neutron energy spectrum at earth depends upon the solar charged-particle spectrum which is given by $dJ/dP = (dJ/dP)_o \exp(-P/P_o)$ where P is the particle rigidity and P_o is the characteristic rigidity which varies from event to event (Freier and Webber, 1963). Differential solar neutron energy spectra for P_o ranging from 60 to 400 MV have been presented by Lingenfelter and Ramaty (1967). If this differential neutron spectrum is taken to be of the form n(E) neutrons/cm^2 sec MeV, then the mean efficiency

is given by

$$\bar{\varepsilon} = \int n(E)\varepsilon(E)dE / \int n(E)dE. \qquad (3)$$

The mean efficiencies for spectra with P_o = 60 MV and P_o = 125 MV are calculated to be respectively 0.38 cm^2 and 0.37 cm^2, about 20% larger than for an isotorpic flux. If neutrons are incident perpendicular to the axis of symmetry, then C = 1. Therefore, at the 95% confidence level, the upper limit to the integral solar neutron flux in the energy range 1-20 MeV is $4.9 \times 10^{-3}/cm^2$ sec for P_o = 60 MV. The neutron energy range is defined by the low-energy shape of the solar neutron energy spectrum which decreases rapidly at lower neutron energies because the survival probability of the low energy neutrons is small.

If there are any solar neutrons, then this upper limit to the measured direct solar neutron flux must be corrected for the atmospheric neutron leakage flux arising from the interaction of solar neutrons with the earth's atmosphere. This correction is carried out as follows. Let the total solar neutron count rate be $N = N_A + N_D$, where the subscript A refers to the contribution from atmosphereic leakage and D to the contribution from solar neutrons directly incident on the detector.

The calculations of Alsmiller and Boughner (1968) for the differential neutron flux (neutrons/cm^2 sec MeV) produce at various depths in the atmosphere by solar flare neutrons can be used to estimate the resulting neutron leakage flux. Then, the corresponding solar neutron fluxes (see equation 2) in the energy interval covered by the OGO-6 detector are: $F_D = N_D/\bar{\varepsilon}_D$ and $F_A = N_A/2\bar{\varepsilon}_A$, since C = 2 for a flux isotropic over a hemisphere. Putting $F_A = a F_D$,

$$F_D = \frac{\bar{\varepsilon}_D}{2a\varepsilon_A + \bar{\varepsilon}_D} \frac{N}{\bar{\varepsilon}_D} \qquad (4)$$

Now, since the OGO-6 detector responds principally to direct solar neutrons with energies 1-20 MeV, $F_D = F_T (\int_0^{20} J(E)\,dE / \int_1^{\infty} J(E)\,dE) = 0.267 F_T$. F_T is the total integral incident solar neutron flux with a differential energy spectrum J(E) given by Lingenfelter and Ramaty (1968) for P_o = 60 MV. The incident solar neutron flux F_T gives rise to an atmospheric neutron source F_N at small atmospheric depths, of which a fraction $r = (F_A{}^T)/F_N$ leaks out of the atmosphere. Of the total solar neutron leakage $F_A{}^T$, the OGO-6 detector responds to a flux F_A from 10 keV-10 MeV. Putting $b = F_A/F_A{}^T$, then F_A (10 keV-10 MeV) $= b F_A{}^T = br F_N = brn F_T = \frac{brn}{0.267} F_D = a F_D$. Assuming the neutron spectral shape

for the leakage flux to be the same as given by Hess et al. (1961), b = 0.94 at the geomagnetic equator for the period in the solar cycle corresponding to that for these measurements. For this spectrum r is estimated to be 5 < r < 10% (Lingenfelter, 1963). Taking the smallest value of n = 1 to yield the highest upper limit to F_D, a = 0.25. For this neutron leakage spectrum $\bar{\varepsilon}_A = 1.35\ cm^2$. Therefore, the corrected upper limit to the quiet time solar neutron flux from equation (4) is

$$F_D = 0.363 \frac{N}{\bar{\varepsilon}_D} = 1.8 \times 10^{-3} n/cm^2 sec.$$

In evaluating the solar neutron leakage flux from the atmosphere the contributions from neutrons with E_n <0.5 MeV were assumed to be given by the spectral shape of Hess et al. (1961). Actually, the spectrum of Alsmiller and Boughner (1968) is still riched in neutrons below 0.5 MeV. For the latter spectrum the upper limit is reached by about 10%. Such an extrapolation is not included in the upper limit placed on the solar neutron flux by the OGO-6 measurements.

The upper limit to the "quiet-time" integral solar neutron flux deduced here is comparable to the value of $\leq 2 \times 10^{-3}\ cm/sec^2$ in the 1-10 MeV range obtained by Hess and Kaifer (1967). Upper limits to the solar neutron

flux have also been set by Zych and Frye (1969), Kim (1967), Forrest and Chupp (1968), and Cortellessa et al. (1971), but at much higher energies from 10 to 200 MeV. For comparison with other measurements the OGO-6 result was converted to a differential flux by folding the energy dependent response function into the shape of the solar neutron energy spectrum calculated by Lingenfelter and Ramaty (1967) for a characteristic rigidity P_o = 60 MV. For characteristic rigidities greater than 60 MV the limiting fluxes will be smaller. These results are shown in Figure 3. Where only integral solar neutron intensities were measured, e.g., Hess and Kaifer (1967), the results have been converted to a differential neutron spectrum using the spectral shape presented by Lingenfelter and Ramaty (1967) and the known energy dependent response functions. At lower energies the OGO-6 result has the lowest experimental upper limit for the continuous emission of solar neutrons in the 1-20 MeV neutron energy range. FIG.3

4. DISCUSSION OF RESULTS

The OGO-6 solar neutron results place a lower upper limit in the 1-20 MeV energy interval and should be interpreted along with the recent higher energy results of Cortellessa et al. (1971), the limits set by Heidbreder et al. (1970) and Eyles et al. (1971), and the earlier

measurements by Webber and Ormes (1967), all of which are shown in Figure 3. In the energy range 20-200 MeV the new limit set by Cortellessa et al. (1971) is within a factor of two of the upper limits previously set, which is very consistent agreement. In fact, no lower limits have been assigned in the 100-300 MeV energy interval than the early ones deduced by Webber and Ormes (1967). Although the calculations of Alsmiller and Boughner (1968) suggest that efficiency used by Webber and Ormes for the production of secondary protons by solar neutrons in the first few grams/cm^2 of the atmosphere might have been 50% too large, the value deduced for the solar neutron flux is still close to these new lower limits because the count rate limits set were very conservative. In the 2-20 MeV the OGO-6 solar neutron results set an order of magnitude lower upper limit than the measurements of Forrest and Chupp (1969) and Coretllessa et al. (1971) in the overlapping energy range.

The lowest measurements in Figure 3 are about comparable to the time-average intensity of the solar neutron flux from the many flares occurring during the last solar cycle 1954-1965 as calculated by Lingenfelter et al. (1965b). At 40 MeV this estimated flux was $\sim 2 \times 10^{-5}$ neutrons/cm^2 sec MeV. Since the solar activity in the present cycle (1965 to $\sim$1974) is considerably less

than the preceding one, the time-average intensity should be considerably less. This time-average intensity is still more than an order of magnitude greater than the theoretical upper limit obtained by Roelof (1966) based upon the IMP-1 protons, assuming all the protons resulted from neutron decays and the protons suffered isotropic diffusion. This suggests that the current measurements are predominately just background measurements. A comparison of the solar neutron flux to the atmospheric neutron flux supports this conclusion. At the geomagnetic equator for neutron energies E_n >50 MeV both the solar and atmospheric neutron spectra have a similar energy dependence and magnitude if Lingenfelter and Flamm (1965) time-averaged values for solar neutrons are used. For $5 < E_n < 50$ MeV the atmospheric neutron flux is two orders of magnitude greater. Indeed, recent atmospheric neutron measurements by Simnett (1971) indicate a spectral shape which is relatively flat from 10 MeV to 50 MeV than decreasing as E^{-2} for E_n >50 MeV. This would make it difficult to separate the two neutron sources by studies of the spectral shape at lower energies.

More meaningful upper limits on the solar neutron flux can only be determined by neutron detectors with much larger geometrical factors, better efficiency and directionality to reduce the background of atmospheric neutrons. Large detecting systems which do not separate

neutron produced events from the background of gamma-ray interactions and other sources cannot provide more significant limits to the solar neutron flux unless detailed statistical analyses of the background counting rates are made to eliminate any possible fluctuations, as does in the analysis of Forrest and Chupp (1969).

Of course, these results do not exclude the possibility that there are neutrons from the sun during solar particle events. Unfortunately, no detecting systems with a high efficiency for neutrons have been aloft during any large solar flare events. In the OGO-6 measurements we looked for solar neutrons during the solar flare events between June and December, 1969. No positive evidence for any neutrons after several solar flares was found. No limits were placed upon the flux because the statistical uncertainty was too large.

We conclude that the quiet-time solar neutron flux from 1-20 MeV cannot be greater than 1.8×10^{-3} n/cm^2 sec at the 95% confidence level. This estimate is based upon a solar charged particle spectrum with a characteristic rigidity P_o = 60 MV.

ACKNOWLEDGMENTS

We gratefully acknowledge the assistance of discussions with Drs. E. L. Chupp and W. R. Webber in various phases of this research program. We thank Ms. S. Dewdney, Mr. A. Buck, and R. Hart for their assistance in computer programming and in performing calculations.

This work is supported by the National Aeronautics and Space Administration under contracts NAS5-9313 and NGR 30-003-008.

REFERENCES

Alsmiller, R. G. and Boughner, R. T. : 1968, J. Geophys. Res. 73, 4935.

Bame, S. J. and Ashbridge, J. R. : 1966, J. Geophys. Res. 71, 4605.

Biermann, Von L., Hazel, O., and Schluter, A. : 1951, Z. Naturfarschg 6a, 47.

Chupp, E. L. : 1971, Space Science Reviews 12, 486.

Cortellessa, P., de Benedetto, P., and Paizis, C. : 1970, Solar Physics 14, 427; Solar Physics 20, 474, 1971.

Daniel, R. R., Gokhale, G. S., Joseph, G., and Lavakare, P. J. : 1971, J. Geophys. Res. 76, 3152.

Eyles, C. J., Linney, A. D., and Rochester, G. K. : 1971, Proc. IUPAP Cosmic-Ray Conf., Hobart.

Forrest, D. J. and Chupp, E. L. : 1969, Solar Physics 6, 339.

Frier, P. S. and Webber, W. R. : 1963, J. Geophys. Res. 68, 1605.

Heidbreder, E., Pinkau, K., Reppin, C., and Schonfelder, V.: 1970, J. Geophys. Res. 75, 6347.

Hess, W. N. : 1962, Proc. of the 5th Intern. Seminar on Cosmic Rays, La Paz, Bolivia.

Hess, W. N. and Kaifer, R. C. : 1967, Solar Physics 2, 202.

Hess, W. N., Canfield, E. H., and Lingenfelter, R. E. : 1961, J. Geophys. Res. 66, 665.

Jenkins, R. W., Ifedili, S. O., Lockwood, J. A. and Razdan, H.: 1971, J. Geophys. Res. 76, 7470

Jenkins, R. W., Lockwood, J. A., Ifedili, S. O., and Chupp, E. L. : 1970, J. Geophys. Res. 75, 4197.

Kim, C. Y. : 1970, Can. J. Phys. 48, 2155.

Lingenfelter, R. E. : 1963, J. Geophys. Res. 68, 5633.

Lingenfelter, R. E., Flamm, E. J., Canfield, E. H., and Kellmann, S. : 1965a, J. Geophys. Res. 70, 4077; 1965b, J. Geophys. Res. 70, 4087.

Lingenfelter, R. E. and Ramaty, R. : 1968, W. A. Benjamin Press, NY, 99.

Lockwood, J. A.: 1972 (to be published), Space Science Reviews.

Lockwood, J. A., Chupp, E. L., and Jenkins, R. W. : 1969, IEEE Trans. Geoscience Electron GE-7, 88.

Roelof, E. C. : 1966, J. Geophys. Res. 71, 1305.

Shea, M. A., Smart, D. F., and McCall, J. R.: 1968, Can. J. Phys. 46, S1098.

Simnett, G. : 1971, Trans. Am. Geophys. 52, 892.

Webber, W. R. and Ormes, J. F.: 1967, J. Geophys. Res. 72, 3387.

Zych, A. D. and Frye, G. M. Jr.: 1969, J. Geophys. Res. 74, 3726.

FIGURE CAPTIONS

Figure 1 - Neutron sensor arrangement and orientation on the OGO-6 spacecraft.

Figure 2 - ^{3}He neutron counter efficiency for an isotropic neutron flux of energy. The details on these measurements are presented by Jenkins et al. (1970).

Figure 3 - Upper limits to the differential solar neutron flux at earth. Not all measured values are shown. For E >50 MeV the upper and lower limits are indicated with a band in which many results not cited lie. The smooth curve marked Lingenfelter and Flamm (1965) is the calculated time-average solar neutron flux at earth for solar cycle 19.

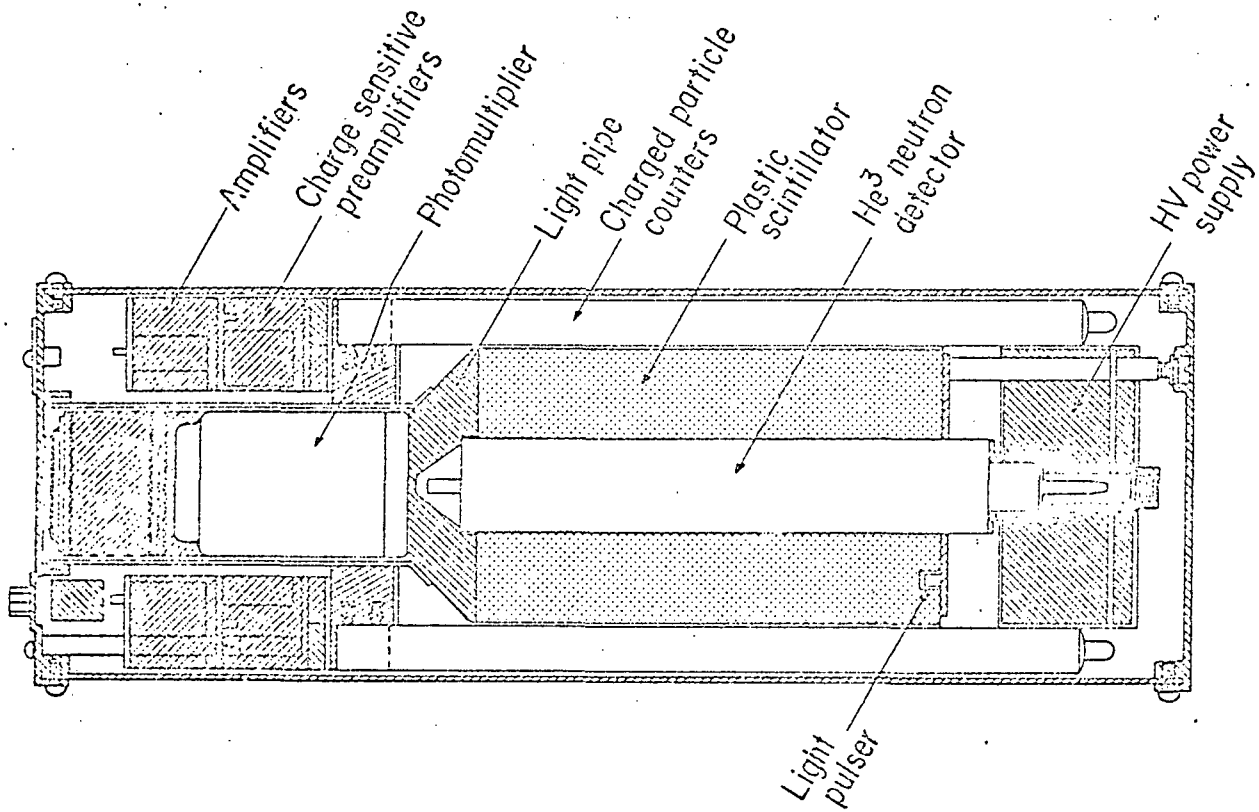

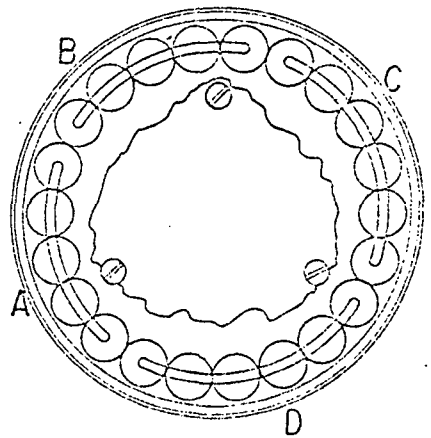

End view of charged particle counters
Coincidence banks
A-C & B-D

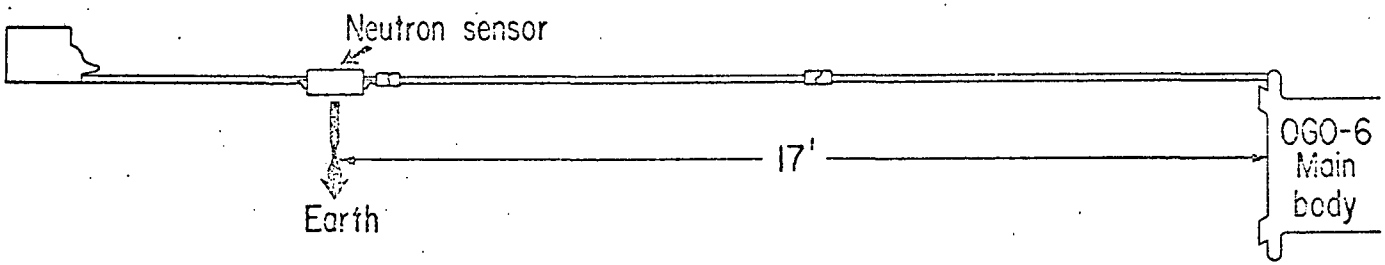

FIGURE 1

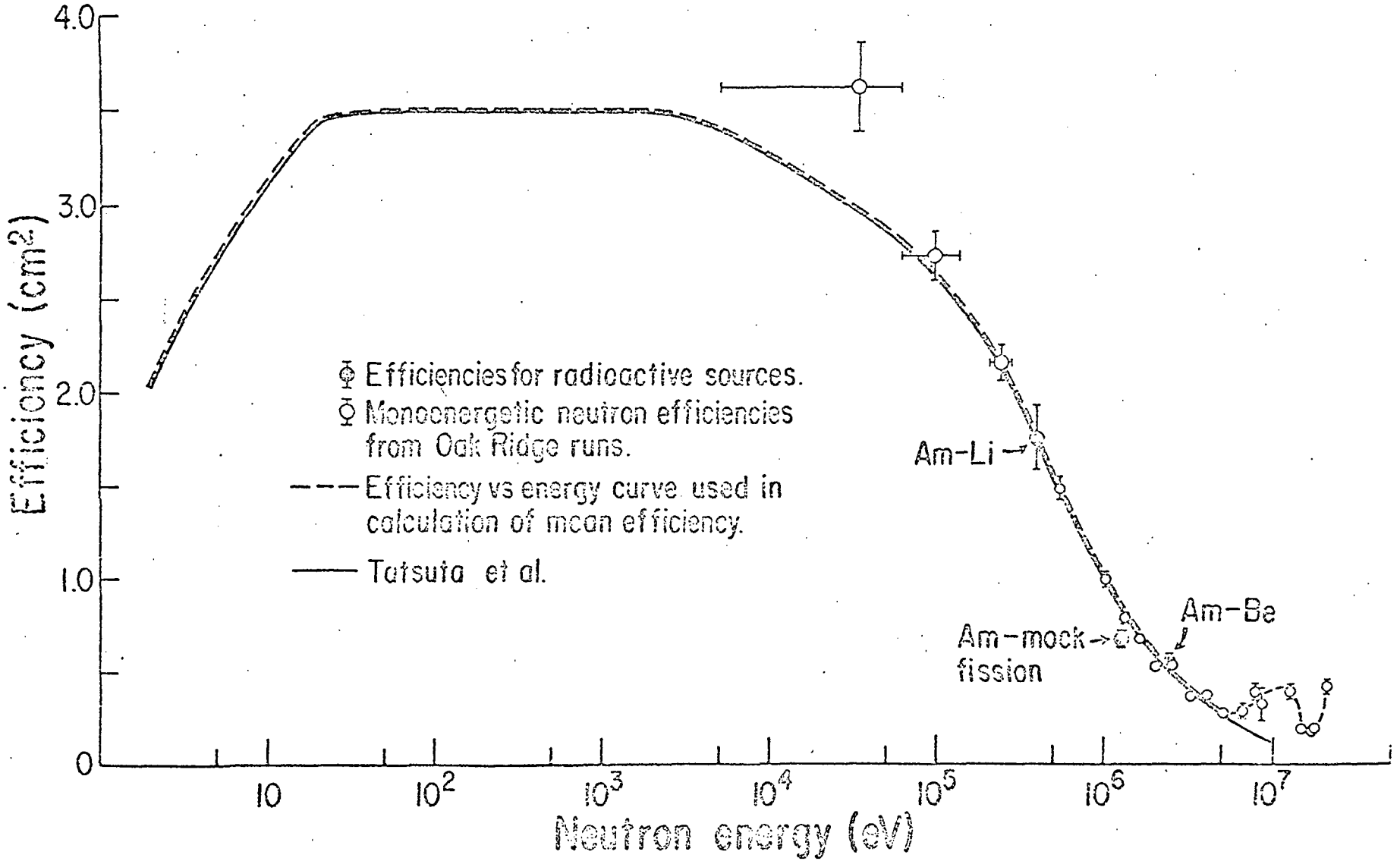
4.0
3.0
2.0
1.0
0
Efficiency (cm²)
Efficiencies for radioactive sources.
Monoenergetic neutron efficiencies from Oak Ridge runs.
Efficiency vs energy curve used in calculation of mean efficiency.
Tatsuta et al.
Am-Li
Am-mock fission
Am-Be
10
10²
10³
10⁴
10⁵
10⁶
10⁷
Neutron energy (eV)

FIGURE 2

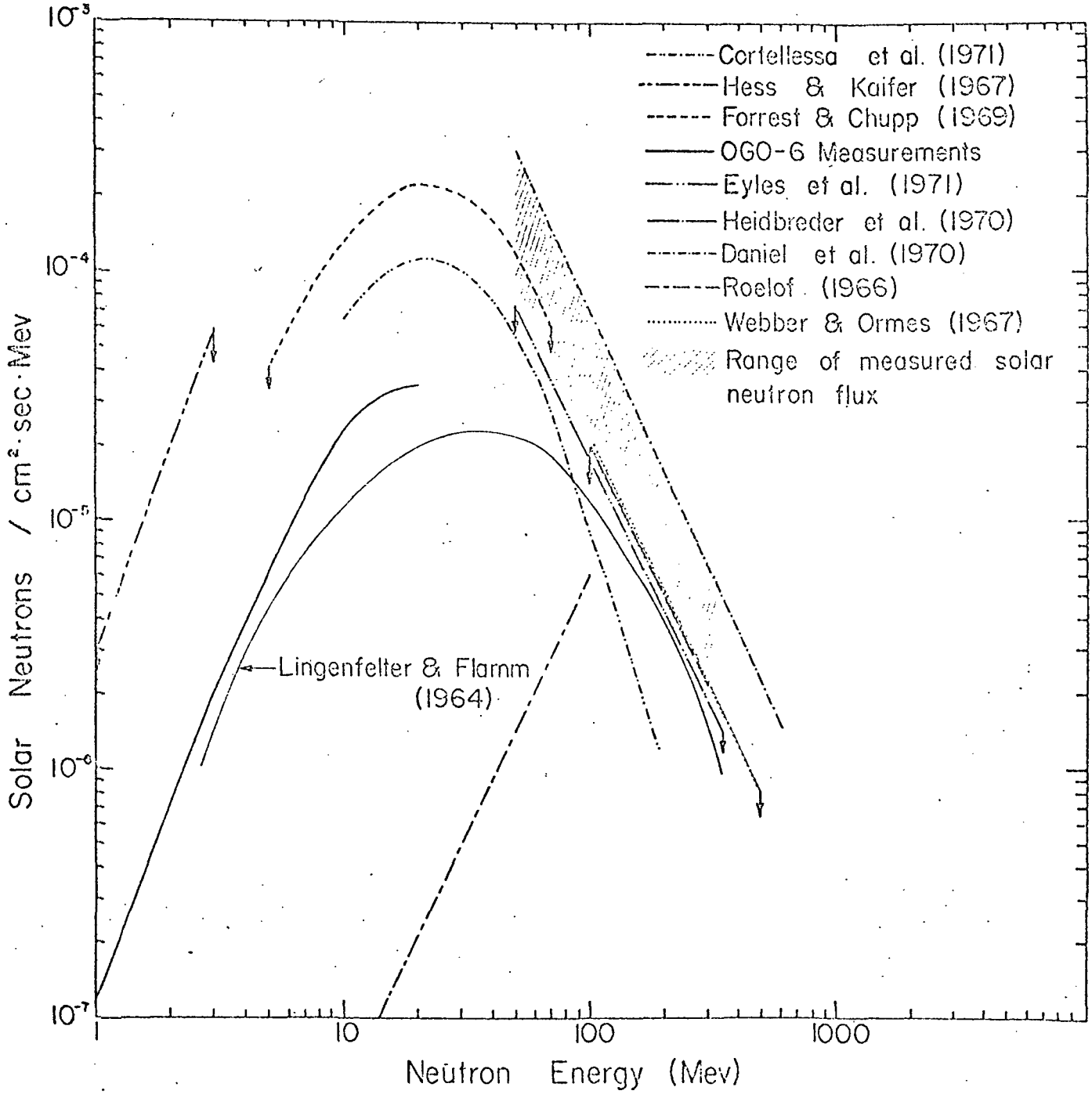
Cortellessa et al. (1971)
Hess & Kaifer (1967)
Forrest & Chupp (1969)
OGO-6 Measurements
Eyles et al. (1971)
Heidbreder et al. (1970)
Daniel et al. (1970)
Roelof (1966)
Webber & Ormes (1967)
Range of measured solar neutron flux
Lingenfelter & Flamm (1964)
Solar Neutrons / cm² · sec · Mev
Neutron Energy (Mev)
10⁻³
10⁻⁴
10⁻⁵
10⁻⁶
10⁻⁷
10
100
1000

FIGURE 3